We thank the anonymous reviewers for their helpful comments on our paper. As detailed below, we have revised our manuscript to reflect their comments, which we feel has resulted in a stronger paper.

Below the reviewer's comments are in boldface, with our responses in plain text. Revised manuscript text is given in italics.

Anonymous Referee #1

This paper describes a closure study that examines the performance of aerosol optical property treatments represented by several models when driven by observed aircraft measurements. Given that climate models have uncertainties in simulating aerosol radiative forcing and chemical transport models are sensitive to radiation via photoloysis rates, this study is important in highlighting deficiencies in models that could be remedied in part by adopting more state-of-the-science treatments of aerosols. The methodology employed is similar to previous closure studies, but as far as I know the models in question have not been confronted with the type of measurements before. Despite the importance of the results of such a closure study, I have several concerns regarding specific details of the approach that affect their conclusions.

Major Comments:

1) A number of times in the manuscript the authors note that computational expense of optical properties as being a reason for simpler approaches employed. It would be useful to be more specific and actually quantify the differences in computational expense of the treatments in the four simpler models versus the ASP model. I have used Mie calculations in 3-D models for many years, and I have never thought of it being a large computational burden compared to other components of a chemistry model. My impression that one reason for many models not adopting new treatments for optical properties is that the scientific community has focused more effort on "hot topics" (e.g. SOA) that overshadow old topics that are viewed as closed and get relatively little attention. In addition there are "simplified" Mie calculations described in the literature.

We agree with the reviewer that on-line Mie calculations are not strictly prohibitive for 3D chemical transport models (CTMs). Rather, as the reviewer notes, given the desires for other model improvements that require additional computations (e.g., increased horizontal and vertical resolution, more chemical species and reactions, etc.), aerosol optical property calculations generally do not get priority for improvements that would require increased computational time. One of the goals of our study was to see if we could justify adding more computationally intensive approaches to 3D CTMs by demonstrating these improvements in ASP. Our results suggest that adding an on-line Mie calculation could help substantially for scattering calculations, but it is less clear that absorption calculations would be improved.

However, we do not think a direct timing test between the simpler models and ASP would be informative of the actual computational differences between the simpler approaches and an on-line Mie calculation, as ASP v2.1 calculates many more wavelengths (every 1 nm from 250 nm to 700 nm) than would be necessary for an on-line Mie calculation. Instead, we have revised our discussion of the relative computational burdens to make clear that the issue is not the absolute time required, but rather the decisions of many modeling groups to invest computational cycles in other processes. See P4, L12-13:

> *However, in order to reduce computational expense (so that the saved computational cycles can be used to increase model resolution, number of chemical species, etc.), most global chemical transport models (CTMs)…*

2) In section there is about a paragraph of information to describe the optical properties used by the four global models used in this study, but I did not get enough information to understand how they compute aerosol optical properties as well as understanding the differences between models. The material seems out of balance with the material presented for ASP. There are two pages of information describing the entire ASP model that has little to do with aerosol optical properties and is really not needed later in the manuscript. I assume that much of the background material on ASP has been described elsewhere and could be greatly shortened. I suggest the entire section be revised to better communicate the methodology of the optical properties for all five models.

Some of the background material on ASP is only available from the thesis of Alvarado (2008) rather than in the peer-reviewed literature, but we agree with both reviewers that it is out of place here and likely unnecessary as the thesis is available online. We have thus cut most of the discussion of the inorganic thermodynamics routines of ASP from the paper.

The optical property calculations of the global models are described in Sections 2.1 to 2.4 of the paper. The methods of OPAC v3.1 and GMI are described in detail, whereas the methods of GEOS-Chem v9-02 and GC-RT are similar to GMI except for the parameter changes noted in Table 1. We have added some text clarifying the methods:

P7, L9-11:

> *For the aerosol components analyzed in this paper (see Table 1), the optical properties are calculated from the assumed log-normal size distributions and refractive indices using Mie theory.*

P8, L10-12:

> *As in GMI, the optical properties for GEOS-Chem v9-02 are based on Mie theory calculations, but with changes to the assumed size distribution, refractive indices, and densities as noted in Table 1.*

P8, L26-27:

> *As in GMI and GEOS-Chem v9-02, the optical properties in GC-RT are based on Mie theory calculations.*

3) There is a lot of scatter associated with closure study for absorption that may have nothing to do with problems in the optical property treatments used in the models. I strongly suggest the authors compare the time series of absorption and black carbon and determine how well those two quantities correlate, and include some subset of this analysis in the paper. One possible issue is that the PSAP may not work well for low concentrations of BC, and if that is the case those data points should not be used in the closure analyses.

We have done the requested comparison for all the data points used in evaluating the fixed size distribution models. The correlation (r^2) between measured submicron absorption at 532 nm and measured submicron BC concentrations is 0.64, indicating a strong correlation (see Figure R1a below). When both data sets are plotted on a log scale (Figure R1b), there is some evidence that the measured absorption is independent of the measured BC concentration for BC concentrations below about 0.03 μg m^{-3} (-1.5 on the x-axis of Figure R1b) which occurs for 261 out of 10,356 data points. However, excluding these points from the analysis does not significantly change the model performance statistics: for example, the slope, r^2, and mean bias for the green channel (532 nm) from GMI stay identical, while the standard deviation of the logarithm of the errors only changes from 0.27 to 0.26 (see Figures R2 and R3 below, and compare with Figures 4a and 5a in the paper).

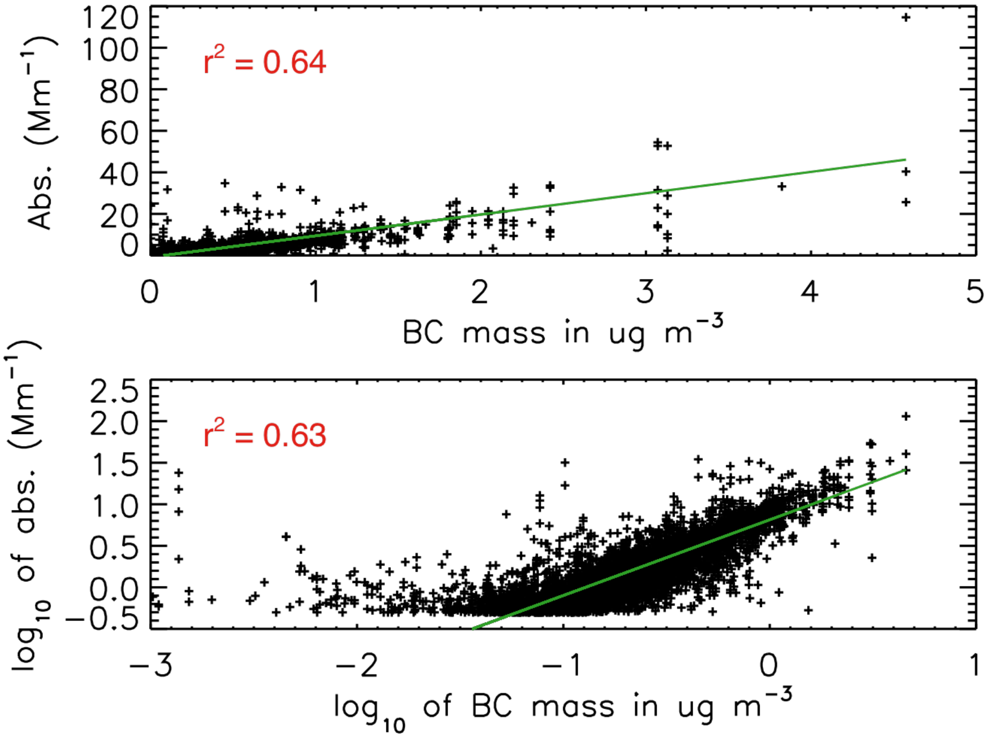

Figure R1. Submicron aerosol absorption coefficients using the Lack et al. (2008) correction versus the submicron BC mass measured using the SP2. The top panel is the absolute units, while the bottom panel shows the $\log_{10}$ of both.

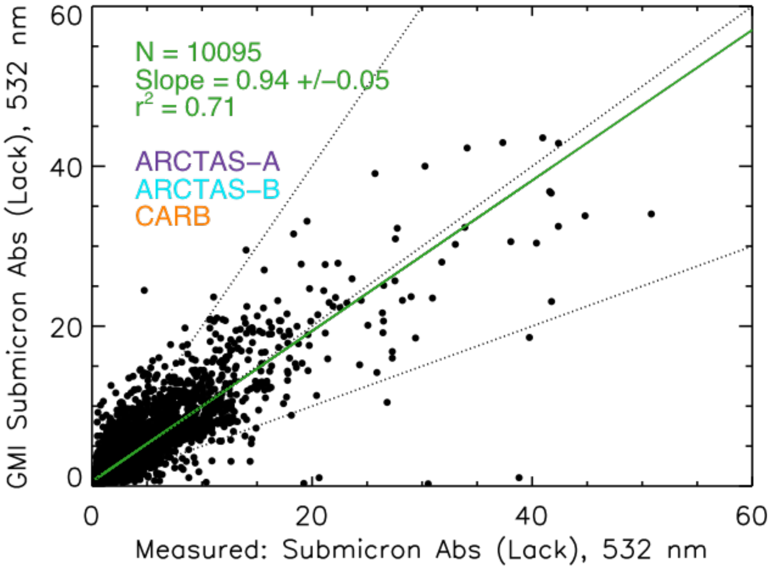

Figure R2. Lack-corrected submicron absorption from the PSAP compared with the GMI model at 532 nm after filtering out data points with a measured BC mass below 0.03 µg m^{-3}.

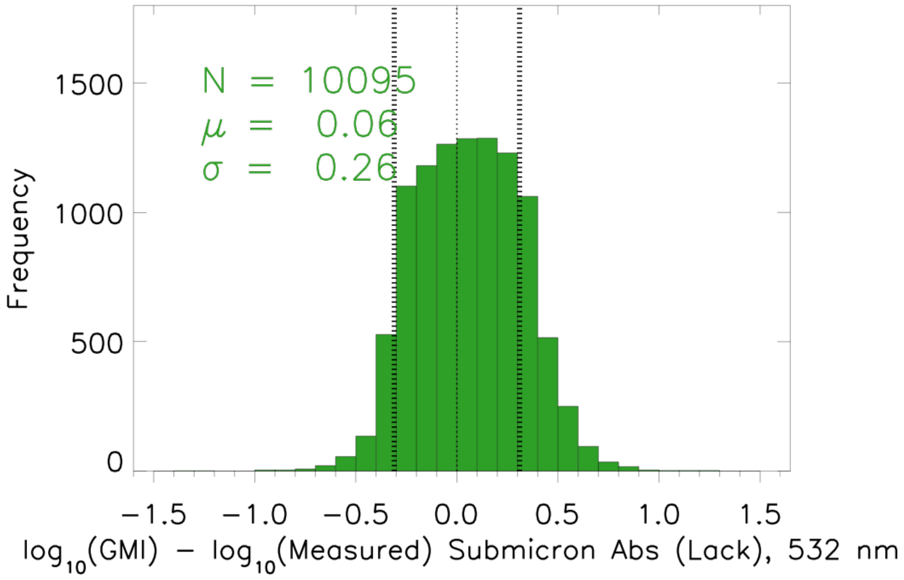

Figure R3. Difference in the logarithms of the GMI and measured submicron absorption at 532 nm after filtering out data points with a measured BC mass below 0.03 µg m^{-3}.

As we have no clear proof that the PSAP measurements are in error at low BC concentrations, and excluding them does not change our results, we prefer to keep these points in our closure study. However, we have added this discussion of potential errors in the PSAP at low BC concentrations to the text (P14, L23-29):

> *The PSAP submicron absorption measurement is well correlated with the submicron BC mass (not shown), with an overall r^2 of 0.64, but the data is uncorrelated for low BC mass concentrations (<0.03 μg m^{-3}), which occurs for 261 out of 10,356 data points in our absorption analysis. However, as we have no clear evidence that these PSAP data points are incorrect and excluding them does not appreciably change the conclusions of our study, we have included these data points in our analysis below.*

4) It would have been useful to propagate some of the measurement and optical property treatment uncertainties into the closure study. Considering the consequences of the measurement uncertainties, and some are no small, are particularly important since the point of the study is to assess how well the model treatments perform.

We agree that including a rough uncertainty propagation would be useful to put the model results in context. Here we thus try to estimate what the errors would be for a hypothetical perfect model.

For the fixed size distribution models, the uncertainties in the inputs are primarily the uncertainties in the mass concentrations from the AMS and SP2. Taking the sum of the squares in the relative standard errors in the mass concentrations of OA (19%), sulfate (17%), nitrate (17%), ammonium (17%), chloride (17%), and BC (30%) gives an overall uncertainty in the inputs of ±49%.

For scattering, the errors in the nephelometer are estimated to be ±1% (Anderson and Ogren, 1998) or ±0.5 Mm^{-1}, whichever is larger. Thus we expect these errors to generally be negligible compared to the errors in the masses except at very small mass loadings. Thus we would expect that a perfect fixed-size distribution model would have an uncertainty of 49% in reproducing the observations. In our evaluation statistics this would correspond to a geometric standard deviation (σ) of 0.17. However, as we are looking at ~10,000 data points, the expected error in the mean is a factor of 100 lower. Thus a perfect model would have a mean (μ) with an absolute value less than 0.01 with a σ of 0.17.

For absorption, the optical measurement uncertainty is at least 30% due to uncertainty in the correct conversion from the filter-based PSAP measurement to the ambient absorption. Here we use the same input uncertainty in the masses, even though the model prediction will be most sensitive to errors in the absorbing components BC and OC. Thus for absorption, a perfect model would have an uncertainty of 57% in reproducing the observations, corresponding to a geometric standard deviation (σ) of 0.20 with a mean (μ) with an absolute value less than 0.01.

For the ASP v2.1 closure studies, the uncertainty in the input size distributions is most important for scattering, with additional uncertainties due to the relative fraction of the different mass components in the aerosol. If we estimate the size distribution using the UHSAS number uncertainty of 20%, then that uncertainty alone would give a geometric standard deviation (σ) of 0.08. Estimating the impact of the relative mass errors is more complicated, as the total mass is constrained here by the size distribution measurements. If we assume the main impact on the scattering uncertainty is the estimated BC mass fraction (30%) and that the uncertainty in the scattering measurement is again negligible, a perfect model would have an uncertainty of 36% in reproducing the scattering observations, corresponding to a σ of 0.13 with a geometric mean (μ) with an absolute value less than 0.01.

For absorption, including the PSAP uncertainty (30%) would mean that a perfect model would have a an uncertainty of 47% in reproducing the absorption observations, corresponding to a σ of 0.17 with a geometric mean (μ) with an absolute value less than 0.01.

Based on this rough analysis, none of the models evaluated in this work are perfect, but it is clear that even a perfect model would have a reasonably large value for σ. We have added this context to the paper in the following places:

P19, L19-27:

> *In order to interpret these closure study results, it is useful to estimate the values of μ and σ we would expect from a perfect model based on the uncertainty in the input mass concentrations and the uncertainty in the scattering measurement. Taking the sum of the squares in the relative standard errors in the mass concentrations of OA (19%), sulfate (17%), nitrate (17%), ammonium (17%), chloride (17%), and BC (30%), as well as the estimated nephelometer uncertainty (1%) gives an overall uncertainty estimate of ±49%, corresponding to a σ of 0.17. Thus even a perfect model would have a fairly significant spread in it's histogram of errors. However, as we are using ~10,000 data points in our comparison, the expected error in μ is about a factor of 100 lower, and thus we would expect $|\mu| \ll 0.01$.*

P20, L15-18:

> *The expected values of μ and σ from a perfect model are $\ll$0.01 and ~0.20, respectively, reflecting the input uncertainties discussed for scattering in Section 5.1 as well as the ~30% uncertainty in converting the filter-based PSAP measurement to the ambient absorption.*

P22, L5-8:

> *…we estimate that a perfect model would have a σ of 0.13 due to the uncertainty in the size distributions and the relative mass contributions.*

P22, L18-20:

> *We estimate that a perfect model would have a σ of 0.17 due to the uncertainty in the size distributions, the relative mass contributions, and in the absorption measurement.*

Specific comments:

Page 2, lines 21-22: "Adding in situ size distribution . . ." sounds awkward to me and should be rephrased. I think what the authors are trying to say is that ASP accounts for aerosol size distribution, but the other models treat aerosols as bulk species with no size distribution? Or is the difference fixed versus variable size distributions?

We were referring to the fact that the four simplified models use fixed size distributions, while ASP has a variable size distribution that in this closure study is matched to the in situ size distribution measurements before calculating aerosol optical properties. We have revised this part of the abstract as follows (P2, L21-24):

> *Adding a variable size distribution, as in ASP v2.1, improves model performance for scattering but not for absorption, likely due to the assumption in ASP v2.1 that BC is present at a constant mass fraction throughout the aerosol size distribution.*

Page 2, lines 24-25: "mixing state" is used here when I think the authors mean mixing rule (as said earlier on line 16). Throughout the text the authors then seem to suggest that these mixing rules are mixing states – and the authors should use language that does not confuse readers. To me whether a model treats complex mixing states has to do more with just the optical properties – it is a fundamental part of how aerosol thermodynamics and dynamics are handled. Simple aerosol models that treat bulk aerosol (either in the simplest external or internal states) can manipulate model parameters using mixing rules (e.g. changing from external state to shell-core) even when that model is not simulating aerosol properties that way. In addition, there are only a limited number of mixing rules that do not reflect the continuum of mixing states.

The reviewer is correct, strictly speaking we are evaluating four different possible mixing rules in ASP, rather than modeling the aerosol mixing state explicitly. However, when we say that further development of ASP should focus on time varying mixing states, here we are referring to the explicit modeling of mixing state. We have clarified this in the abstract (P2, L24-27) and elsewhere in the revised manuscript.

Page 3, line 30: The authors state that the direct effect is uncertain which is true, but the uncertainties in the indirect effect are far larger and are of more concern the climate modelers.

We agree the uncertainties in the indirect affect are larger, but the uncertainties in the direct effect are not yet negligible. We have added the following statement to the end of this paragraph to clarify this (P4, L6-9):

> *While these uncertainties in the aerosol direct effect are generally smaller than the uncertainties in the forcing due to aerosol-cloud interactions (the indirect effect), they are still a significant cause of differences between climate models.*

Page 4, line 9: Change "intensity" to "expense".

Done.

Page 4, lines 29-31: Those conclusions are drawn using data collected during dry conditions and my not apply under higher RH.

We thank the reviewer for noting this, and have added the following sentence to this paragraph (P5, L2-4):

> *However, these observations were made under dry conditions and thus the result may not apply at higher RH.*

Page 5, lines 14-16: I assume that a combination of these factors also contribute to the errors?

We agree that interactions between these factors may also contribute to these errors, and have revised the text accordingly (P5, L19-21)

> *…to help determine if the errors in the global model routines are primarily due to their fixed size distributions, assumptions about external mixtures, their assumptions about the refractive indices of LAC, or interactions between these assumptions.*

Page 11, line 18: The authors mention the UHSAS instrument, which is an optical counter measurement that depend on an assumed refractive index (non-absorbing) that may not be representative of the ambient conditions being measured (see Kassianov et al. Atmosphere, 2015). But the authors do not describe whether the ARCTAS data has been corrected for this artifact. The authors should determine if the data has been corrected and describe some of the uncertainties in the measurements that will affect their closure study.

We agree with the reviewer that the actual refractive index of the particles may be different from the polystyrene latex spheres used to calibrate the UHSAS. Kassianov et al. (2015) present a method for accounting for the effect of the refractive index differences by correcting the size distributions from the UHSAS using an average RI calculated based on the measured aerosol composition. This correction was not applied to the ARCTAS archived data set, and thus the size of the particles may be underestimated in the UHSAS, thereby underestimating the scattering. While this error might impact our results, Figure C2 in Kassianov et al. (2015) suggests that this correction is relatively small for the submicron aerosol of interest in this study. Furthermore, since refractive indices are one of the parameters we are attempting to evaluate, we would need to pick one of the model's assumed refractive indices to perform the correction, which would give that model an advantage in the intercomparison. Thus we have decided instead to discuss this uncertainty and the potential impacts in our paper (P13, L12-17):

> *Note that, as the UHSAS is an optical instrument, it can give incorrect size information if the refractive index of the particles is far from that of the polystyrene latex spheres used for calibration. This artifact can lead to a small underestimate of the size of submicron particles when it is not taken into account, thereby leading to an underestimate of scattering (e.g., Kassianov et al., 2015). However, we expect that this effect on our study will be small relative to the stated precision of the UHSAS.*

Page 12, lines 1-2: A reference is needed for these measurement uncertainties. Measurement uncertainties quoted in the literature for the AMS instrument varies widely, unfortunately.

The quoted uncertainties are those given in the NASA ARCTAS archive data files. The full statement is:

> UNCERTAINTY: Accuracy estimate (2sdev): Inorganics 34%, Organics 38%, dominated by uncertainty in the particle collection efficiency due to particle bounce (Eb, see Huffman et al., Aerosol Sci Technol. 39, 1143-1163, 2005). Precision at low concentrations is the same as the detection limits reported below. Precision at higher concentrations is much better than the accuracy. The accuracy estimates are likely conservative, and may be reduced when a more complete uncertainty analysis of the AMS ARCTAS dataset is completed.

To address this comment, we have added the Huffman et al. (2005) reference, as well as a reference to the Cubison et al. (2011) paper using the ARCTAS AMS data and Bahreini et al. (2009) (P11, L30).

Page 12, line 28: The statement regarding the aerosol mass to be dominated by OA and BC is strange. BC is usually very small, except in the center of biomass plumes. I would still expect sulfate to be a large fraction of mass. In fact, the AMS measurements should tell you whether there is significant sulfate (or nitrate and ammonium too) or not.

We agree with the reviewer – although the biomass burning aerosol sampled in ARCTAS-B are generally dominated by OC and BC, this is not always true for the ARCTAS-A and ARCTAS-CARB campaigns, where sulfate can be a significant fraction of the aerosol mass. What we were trying to say is that we don't expect that minor errors in our estimates of the concentrations of refractory cations from our procedure for matching the SAGA and AMS observations will make a substantial difference, as we expect that most of the aerosol mass is already accounted for by the SP2 and AMS measurements. We have revised the text to make this clearer (P12, L27-30):

> *However, as we expect the aerosol in the ARCTAS campaign to be dominated by the species measured by the AMS and the SP2, errors in our estimates of the submicron refractory cation mass should have little impact on our closure study results.*

Page 13: end of Section 3.2: I would like to see a figure showing the merged size distribution and the individual size distributions from the SMPS, UHSAS, and APS. The critical part is merging these distributions where they overlap. I suspect that at individual times, the overlap might have large disagreements – but that when the data is averaged over a period of time those disagreements likely become smaller.

The method we used to combine the size distributions is described in Section 4.2 of the paper. Figure R4 below shows an example surface area size distribution for a single time point. The surface area distribution is shown here and used to fit the modes for ASP as scattering and absorption are expected to be functions of the particle's cross-sectional area. The "combined distribution" in the dashed line is constructed as described in the text, with the UHSAS data used for diameters between 60 nm and 850 nm, scaled SMPS data used for smaller sizes (with the scaling based on a regression of the points where the SMPS and UHSAS overlap) and with the decay of number concentration for diameters above 850 nm determined by a power-law fit to the APS data assuming a conversion factor of 0.8. We used the UHSAS as our primary source of size distribution data as it is most sensitive to the optically active submicron particles of interest in this study. Our study is less sensitive to the SMPS data (as the particles below 60 nm scatter and absorb relatively little light) and the APS data (as we focus on the optical properties of submicron aerosol).

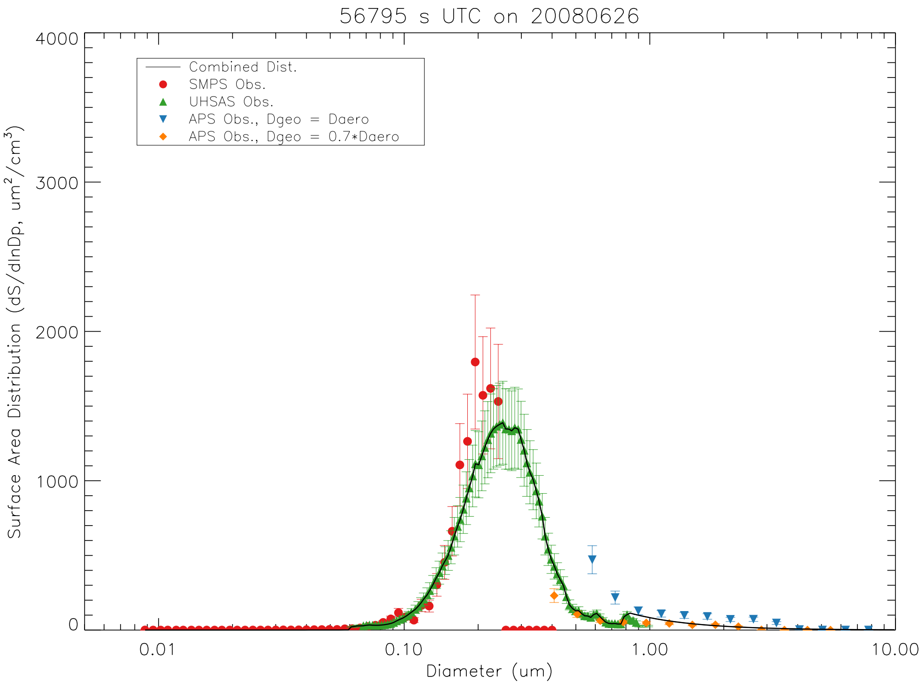

Figure 4. Plot of the surface area distribution (µm^2 cm^{-3}) from the SMPS (red circles), UHSAS (green triangles), and APS (blue triangles for a correction factor of 1.0, yellow diamonds for a correction factor of 0.7) with the combined size distribution plotted as a black line.

Page 14: Section 3.3: More discussion is needed regarding the uncertainties in the scattering and absorption measurements. For PSAP, there have been a number of studies pointing out some of the flaws with the instrument.

As noted in the text, the precision of the nephelometer was 0.5 Mm^{-1} and the precision of the PSAP is 0.2 Mm^{-1}. The paper of Anderson and Ogren (1998) suggests that in practice the actual reproducibility of scattering measurements with a TSI model 3563 nephelometer is ±1%, so we have modified the text to reflect this uncertainty (P14, L8-11)

> *These total scattering coefficients were then corrected for truncation errors using the procedure described by Anderson and Ogren (1998), who report a measurement reproducibility of ±1%. Thus the actual uncertainty in the scattering meaurements is ±1% or ±0.5 Mm^{-1}, whichever is larger.*

In addition, we agree that, as a filter-based absorption measurement, the PSAP has some additional flaws in estimating the in situ absorption of aerosols, and as we discuss, the difference between the two corrections used in the ARCTAS study can differ by 20-30%, which is likely closer to a true estimate of the uncertainty in the absorption measurement. We have edited the text to reflect this (P14, L21-22):

> *Thus the practical uncertainty in the absorption measurement is estimated as at least 20-30%.*

Page 17, lines 1-8: More description is needed on how the aerosol composition is used. I understand the size distributed AMS data is either not available or it may not be desirable to average the optical property measurements over an hour period. But the size distribution for organic matter, sulfate, nitrate, and ammonium may not be the same. If they are assumed to be the same this is an important piece in the methodology to mention.

The size distribution of these compounds is assumed to be the same in the ASP simulation, as suggested above, and we agree with the reviewer that this should be made clear in the methodology. We have addressed this by adding the following sentence to the end of this paragraph (P17, L22-24).

> *This implicitly assumes that the size distributions of all aerosol components (BC, OC, and electrolytes) are the same, which may not have been true in the ambient atmosphere.*

Page 18: lines 23-30: I do not see where data for the 450 nm channel are presented.

These results are given in Table 2, but that was ambiguous in the text. We have added a reference to Table 2 closer to this section in the revised paper (P19, L9).

Page 20, lines 3-16: There are studies that suggest that uncertainties in SSA needs to be very small to have confidence in radiative forcing estimates. The results from this study show that even with the observations we cannot achieve this (large amounts of scatter). So what does this mean for climate model calculations that will have even larger errors in size, composition, and mass? Some perspective on SSA accuracy needed for climate models based on from other studies needs to be discussed.

We agree that our results suggest that the instrumentation used in the ARCTAS campaign is not sufficient to constrain the aerosol SSA to the accuracy needed for climate studies, mainly due to the uncertainty in aerosol absorption. This points to the need for further development of instruments that can measure the absorption properties of aerosols in situ.

We also agree that additional model errors beyond the optical property calculations examined here, from processes such as emissions, chemistry, deposition, etc. could significantly increase the errors in aerosol scattering and absorption calculations in climate models. However, in situ data are not the only data available to constrain the direct radiative effect of aerosols in global models – as noted in our Introduction, AERONET data as well as a variety of satellite instruments (e.g., MODIS) have been used to constrain the net radiative effect of aerosols in these models.

In addition, we agree that some context on the needed accuracy in SSA for climate models would be helpful in interpreting our results. We have thus added the following text to our revised paper (P21, L7-11):

> *Note that the size of the uncertainties in SSA seen in Table 4 can have a significant impact on estimates of global aerosol DRF. For example, Loeb and Su (2010) found that a SSA perturbation of 0.03 over land and 0.06 over ocean could lead to errors in all-sky DRF of -0.73 to +1.11 W m^{-2}.*

Page 22, line 7: The authors suggest that BC is expected to be externally mixed for fresh smoke. I suggest the authors actually provide evidence for this. A number of studies have shown that SP2 can be analyzed to produce coating thickness as a function of size. If the authors are correct then the coating thickness should be small to zero when the aircraft is sampling in fresh smoke, and larger thickness further downwind. Is coating thickness available from the ARCTAS SP2 measurements?

We do not think that the statement that fresh smoke aerosols are more externally mixed than aged smoke is very controversial, but we do agree we should have provided better references for this claim. For example, Akagi et al. (2012) found that the fraction of BC particles classified as “thickly coated” in the SP2 analysis of a California chaparral fire increased from a value of 0.55 to ~0.80 over four hours of aging. The Colockum Tarp fire sampled during the 2013 Biomass Burning Observation Project (BBOP) also showed a rapid increase in the fraction of thickly coated BC (Sedlacek et al., presentation at the 2014 ASR Science Team Meeting, http://asr.science.energy.gov/meetings/stm/2014/presentations/ASR-talk-20140310.pdf).

Examining the SP2 coating thickness versus smoke plume age would be well beyond the scope of this study. However, to address this comment we have looked at the coating thicknesses in the quasi-Lagrangian sampling of the Lake McKay fire from ARCTAS-B (Alvarado et al., 2010; Cubison et al., 2011) using the median value of the shell/core ratio only for Black Carbon particles with core diameter range of 170-300 nm, which is provided in the ARCTAS data archive. The results are shown in Figure R5 below, and suggest an increase in coating thickness in the first half hour of plume aging.

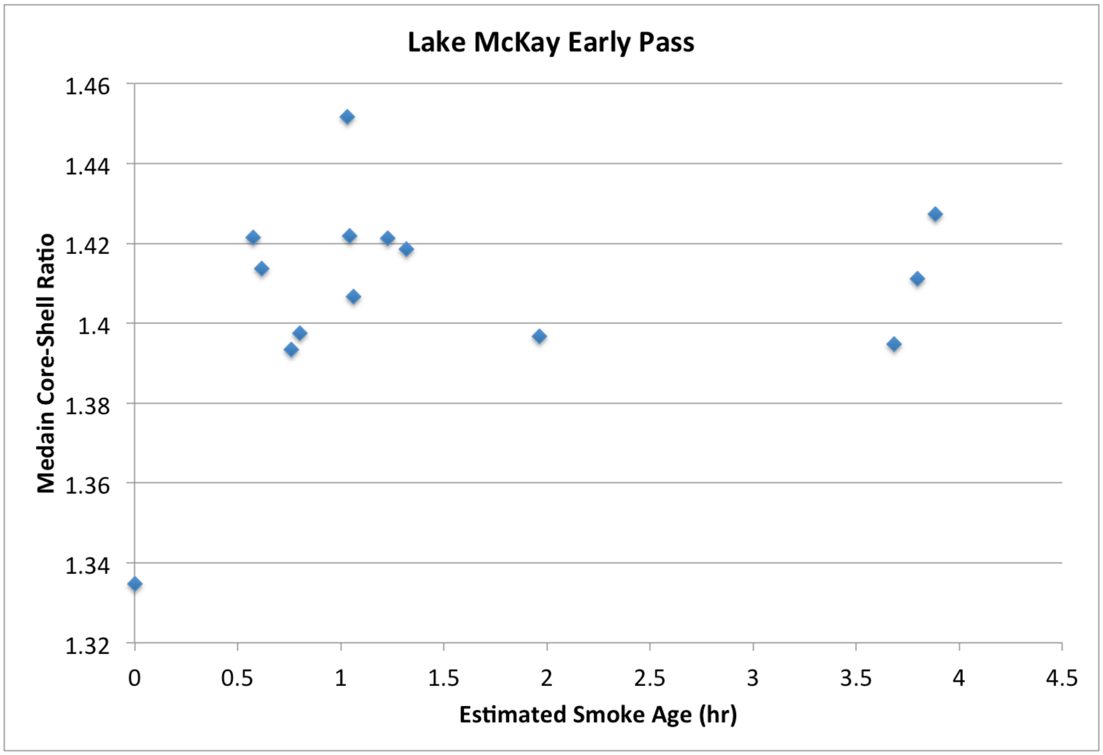

Figure 5. Median core-shell ratio for coated BC particles with core diameters between 170-300 nm versus estimated smoke age for the early pass of the Lake McKay fire in ARCTAS-B.

However, given that even in fresh smoke about half of the BC particles can be classified as "thickly coated", we agree that our statement in Section 6.2 is too strong. We have thus modified the text (P23, L10-13):

> *In contrast, ARCTAS-B sampled substantial amounts of fresh biomass burning smoke, where about half of the BC would be expected to be externally mixed (e.g., Akagi et al., 2012) and thus have lower absorption per mass of BC than would be calculated by the core-shell assumption.*

Page 22, line 13: I do not think enough proof is provided regarding mixing state in the observations.

We agree that the observations do not provide definitive proof that changes in mixing state are responsible for the differences between the three ARCTAS campaign. We have thus softened the language in the revised paper (P23, L17-21)

> *These results do not definitively prove that the difference in the performance of ASP v2.1 for the three ARCTAS campaigns is due to errors in mixing state, but they do suggest the need for further development of the ASP model to allow for time-varying mixing states and to allow the BC size distribution to vary independently of the overall size distribution.*

Page 22, line 26: Table 7 is presenting the results by mixing rules, not mixing state.

Agreed, this has been changed to mixing rule in the revised manuscript (P21, L30 and elsewhere).

Page 24, line 12 and 20: I do not think the model does a reasonable job in absorption, contrary to what the authors state in line 12. Then in line 20 the authors state that there should be improvements in absorption – a contradiction in this paragraph.

The statement in Line 12 referred to the GMI model, while the statement in line 20 referred to ASP, which performed worse in absorption than GMI, so the statements are not inconsistent. However, we agree that we may have overstated the performance of the GMI model here. We have modified this as follows (P25, L8-11):

> *These results suggest that the GMI model performs the best of the four fixed size distribution schemes evaluated here in simulating submicron aerosol scattering and absorption, and that future refinements to the GMI approach should focus on improvements that, on average, reduce scattering and absorption in the 550/532 nm and 450/470 nm bands.*

Reviewer 2

This paper presents a closure study using in situ observations of aerosol composition and size as well as aerosol optical properties during the ARCTAS campaign to validate five aerosol optical properties modules. During this campaign there was a large abundance of biomass burning aerosol, so the focus of this closure study is on absorption. Four of those modules have in common that they prescribe the aerosol size distribution parameters, so the aerosol mass concentrations are the only inputs. These modules are used in current global models. The fifth optical properties module is used as part of the more detailed aerosol process model ASP and can make use of size distribution information.

I regard this paper as a valuable contribution to isolate and quantify errors in optical properties calculations that are part of state-of-the art models. I have some questions and suggestions that would make the presentation of this paper clearer. I recommend this paper for publication after these are addressed.

General comments
1. Closure studies of optical properties have a long history. I encourage the authors to shift the emphasis in the introduction from describing the importance of LAC to reviewing some of the closure studies in the literature to provide context for the work under review. A few examples are Cai et al., 2011, Highwood et al., 2012, Esteve etal., 2014, Quinn and Coffman, 1998, Sciare et al., 2005, Wex et al., 2002, but there are many more.

Cai et al., Journal of Geophysical Research, 116 (2011), D02202
Highwood et al., Atmospheric Chemistry and Physics, 12 (2012), 7251–7267
Esteve et al., Atmospheric Environment, 89 (2014), 517- 524
Quinn and Coffman, Journal of Geophysical Research, 103 (1998), 16575–16596
Sciare et al., Atmospheric Chemistry and Physics, 5 (2005), 2253–2265
Wex et al., Journal of Geophysical Research, 107 (2002), 8122

We agree, and thank the author for pointing our attention to the above references. While we still think the discussion of LAC in the introduction is also useful for illustrating the motivation for the work, we have added a discussion of these previous closure studies to our revised paper.

P5, L22 to P6, L5:

> *Previous closure studies have looked at both the scattering and absorption of aerosols measured at surface sites (Sciare et al., 2005; Cai et al., 2011), from research vessels (Quinn and Coffman, 1998) and from aircraft (Wex et al., 2002; Cai et al., 2011; Highwood et al., 2012; Esteve et al., 2014). For example, Quinn and Coffman (1998) found agreement in the submicron scattering calculated via a Mie code using the in situ size distribution and composition measurements and measurements from an integrating nephelometer to within measurement*

> *uncertainty, but did not get good agreement for supermicron aerosol. More recently, Highwood et al. (2012) used a Mie code to simulate aerosol scattering (450, 550, and 700 nm) and absorption (567 nm) for several aircraft flights during the EUCAARI-LONGREX campaign, finding agreement within the measurement uncertainties of 30%. Esteve et al. (2014) expanded on this work by using a flexible Mie code assuming homogeneous internally mixed spheres. They found that the agreements between the calculation and measurements of absorption and scattering was within measurement uncertainties for EUCAARI-LONGREX, as in Highwood et al. (2012), but that there was poorer agreement for the VOCALS-Rex campaign, where detailed in situ observations of the aerosol size distribution were not available.*

P6, L14-17:

> *This study differs from the closure studies discussed above in that these aerosol optical property modules, which simulate the aerosol as an external mixture of different components each with mixed size distributions, are evaluated directly without the additional constraints provided by the measured aerosol size distributions.*

2. The description of the models/ aerosol optical property modules is somewhat confusing. I recommend referring consistently to the actual optical property module in each case, since the full chemical transport models are not used for this study. For example, in section 2.2, what is actually evaluated is a portion of the FAST-JX model, correct? Similarly, large parts of section 2.5 seem to be not relevant for this paper, as there are no model runs using the full ASP model, but only the optical properties module is used. If that's indeed the case, I recommend eliminating or substantially shortening section 2.5.1, except for the description about the assumptions how aerosol composition is represented over the different size bins.

We agree with the reviewer's comment. As noted in the response to Reviewer #1, we have cut most of the extraneous information from Section 2.5.1 as requested. Also, for GMI, GEOS-Chem v9-02, and GC-RT, we are in fact comparing the optical properties that each model feeds into the FAST-JX subroutine for radiative transfer calculations, but as these inputs are different for each model, we think it is simplest to identify them using the name of the host CTMs in which they are used.

Specific comments

1. Replace the phrase "to get" with "to obtain" (e.g. line 5)

Done – see P4, L5 and elsewhere in the revised text.

2. page 4, line 9: replace "intensity" with "burden" or similar

We have changed it to “expense” as recommended by Reviewer #1. See P4, L12 in the revised text.

3. page 5, line 2: should read “result”

Done – See P5, L7 in the revised text.

4. page 6, line 7: suggest to rephrase: “six types of water clouds, three types of ice clouds and ten aerosol types”

Done – See P6, L31 in the revised text.

5. page 6, line 12: The list of different components is confusing. Is water-insoluble aerosol everything insoluble except for soot and mineral dust (which are a separate class), and is water-soluble aerosol everything soluble except for sea salt and sulfate? Please clarify.

We agree that the terminology used in OPAC v3.1 to describe their aerosol components is confusing. Hess et al. (1998) states that the water-insoluble component “consists mostly of soil particles with a certain amount of organic material), while the water-soluble component “consists of various kinds of sulfates, nitrates, and other, also organic, water soluble substances.” In practice, most global models use the water-soluble class from OPAC as a starting point for their model of organic carbon (OC) and do not include the water-insoluble class.

We have clarified this in the revised text (see P7, L5-9):

> *The aerosol components included are “water-insoluble” aerosols (primarily soil particles), water-soluble aerosols (primarily organics and other secondary aerosol components, see Hess et al., 1998), soot, two size modes of sea salt, four size modes of mineral dust, and sulfate droplets. A given aerosol is then modeled as an external mixture of these ten aerosol components.*

6. page 6, line 30: should read “based on Mie theory calculations” (remove “the”).

Done, see P7, L26 in the revised text.

7. page 7, line 1: How is dependence of refractive indices on relative humidity parameterized?

As most of our measurements are at very low RH, the dependence of the aerosol optical properties on relative humidity is not very important for our study. However, we agree that we could describe it better in the text. Following OPAC, in most of the fixed-size-distribution models some of the aerosol species are assumed to take on water with increasing RH following prescribed growth curves. The resulting refractive index is then calculated as a volume weighted mixture of the dry aerosol species and water.

We have added this discussion to the text (P7, L28-29):

> *The relative humidity dependent complex indices of refraction (calculated using a simple volume-average mixing rule, see Hess et al., 1998)…*

8. page 8, line 24: suggest to rephrase: "all particles in a size bin are assumed to have the same composition".

Done, see P9, L22 in the revised text.

9. Page 8, line 26: suggest to rephrase: "one bin each for particles smaller than 10 nm or larger than 20 µm."

Done, see P9, L25-26 in the revised text.

10. page 8, line 28: This sentence says that the mass fractions of different aerosol components are the same for all the bins. Does this mean that the aerosol is assumed to be fully internally mixed? In other words, it's not only assumed that the particles within one bin have the same composition as stated two lines above, but all particles have the same composition?

Yes, all size bins are assumed to have the same relative composition. We have edited the text to make this clearer (P9, L27-29):

> *In ASP v2.1, the mass fractions of different aerosol components are assumed to be independent of aerosol size, so the relative aerosol composition is the same in each size bin.*

However, the statement above that all particles within a size bin have the same composition is not true when the external mixture (EXT) mixing rule is used, as in that case we assume that the particles are either pure BC or internal mixtures of the other components. We have thus edited this text to make that clear (P9, L20-23):

> *In this representation, size bin boundaries remain fixed while the mean particle size within the bin is allowed to change with time, and all particles in a size bin are assumed to have the same composition (except when the external mixture (EXT) mixing rule is used, see Section 2.5.2).*

11. page 10, line 27: Regarding the Maxwell Garnett mixing rule, are there assumptions necessary how many BC inclusions there are, if so, what is assumed in this study?

As we are dealing with small particles where there is likely only a single BC inclusion, that is what we have assumed in this study for the Maxwell Garnett mixing rule. This is in contrast to cloud droplets, which could potentially have several BC inclusions. We have clarified this in the text (P10, L19-21):

> *…the Maxwell Garnett (MG) mixing rule, which here assumes that BC is present as a single randomly distributed inclusion within the particle (Maxwell Garnett, 1904);*

12. page 11, line 22: The SP2 instrument only covers a range above 90 nm, but a fraction of BC particles will have smaller cores, which will be missing from the mass concentration, but their absorption will be captured. Can you estimate how big of a problem this is for the closure?

We agree with the reviewer that this could be a problem. However, this would tend to result in the models under-predicting absorption relative to observations, as a perfect model would have too little BC to represent the measured absorption. However, we found that nearly all models were overestimating absorption, with the exception of ASP v2.1 using the EXT mixing rule at the 470 and 532 nm wavelengths. Thus this error would tend to make the models match observations more closely than they should.

We can make a more quantitative estimate of the effect by estimating the amount of BC mass with diameters below 90 nm. Using the OPAC, GMI, GEOS-Chem v9-02, and GC-RT size distributions for BC gives ~10% of the total BC mass below 90 nm. Thus we expect this missing BC mass would bias the models low in absorption by about 10%. This is less than the SP2 uncertainty (30%), but would be a near constant effect. However, we'd expect it to have less of an influence on our closure study than the differences in the filter corrections for the PSAP.

We have added this discussion to the revised text (P11, L16-22):

> *As a rough estimate, we calculate that by not measuring the BC mass below 90 nm, using the measured SP2 mass could bias a perfect absorption model low in absorption by about ~10%. However, as shown in Section 5 and 6, most models studied here overestimate submicron aerosol absorption, so this potential bias would tend to move the models closer to the observations. In addition, this bias is smaller than the potential bias in the absorption measurements due to the filter corrections, as noted in Section 3.3.*

13. page 13, line 13: replace slower with lower.

Done, see P13, L19 of the revised text.

14. page 13, line 19: should read 7.75 ?

This should have read 7.75 µm – we have fixed it in the text (P13, L24).

15. Section 4.1: Since size distribution measurements are available, can you include some information of how close/how different the observed size distributions were from the assumed distributions?

The assumptions used for size distributions in most of these the fixed size distribution models are not selected because they are expected to closely match in situ size distribution measurements, but that they are expected to give reasonable aerosol optical properties under a wide variety of condition. Thus we feel that a rigorous comparison of the measured size distributions with the assumed ones for these models would require significant additional work and would be unlikely to provide much benefit.

16. page 15, line 16: add "volume" to "extinction coefficient"

Done, see P15, L29 of the revised text.

17. page 16, line 26: here the authors talk about modes as inputs for ASP, which is in contradiction to the information on page 8, which talked about size bins. Please clarify.

The issue is that while ASP v2.1 represents the aerosol size distribution using a sectional size distribution, the routines used in ASP v2.1 to initialize this aerosol distribution currently only allow input of an arbitrary number of log-normal aerosol modes which are used to populate the size bins. Thus the combined size distribution has to be represented using log-normal models for input to ASP, but the optical properties are calculated based on the properties of the size bins.

We have clarified this in the revised text (P17, L8-12)

> *While ASP v2.1 represented the aerosol as a sectional size distribution as described in Section 2.5.1, the initialization routines of ASP v2.1 require that the dry aerosol size distributions be input as a sum of lognormal modes which are then used to populate the size bins. Thus the "combined" size distribution described above is fit to three lognormal modes (see Equations 13.18 and 13.20 from Jacobson, 2005).*

18. page 19, line 2: delete "the shows"

Done, see P19, L29 of the revised text.

19. Section 6: the term mixing state is used when it should be mixing rule.

The reviewer is correct, strictly speaking we are evaluating four different possible mixing rules in ASP, rather than modeling the aerosol mixing state explicitly. However, when we say that further development of ASP should focus on time varying mixing states, here we are referring to the explicit modeling of mixing state. We have clarified this in the abstract (P2, L24-27) and elsewhere in the revised manuscript.

20. Conclusions: The four fixed-size-distribution models are all rather similar. Can you comment on why the GMI leads to the best results?

The differences between the four fixed-size distribution models seem to be primarily due to the assumed size distributions and densities of the aerosol components, rather than due to the assumed refractive indices. The simplest comparison is between GMI and OPAC v3.1, as they have the same refractive indices for all species considered here. In terms of absorption, the most significant difference is the assumed density of BC, which is 1.0 g cm^{-3} in OPAC v3.1 and 1.5 g cm^{-3} in GMI, with the assumed size distribution of BC the same in both models. The higher density for BC reduces the volume and cross-sectional area of the BC particles per unit BC mass, reducing the calculated absorption and thus reducing the positive bias for absorption. This improvement is partially offset by the lower density for OC (the other absorbing component). GEOS-Chem v9-02 uses the same refractive index and density for BC and OC as OPAC v3.1, but the larger mode radii and smaller standard deviations of the size distributions result in stronger absorption at 470 nm. In GC-RT, the increase in absorption due to the increase in the imaginary refractive index for BC is offset by the increase in the BC density to 1.8 g cm^{-3}.

We have added some of this discussion to the conclusions:

P24, L18-21:

> *The better performance of GMI for absorption seems to be primarily due to the assumption of a larger density for BC (1.5 g cm^{-3}) than in OPAC v3.1, as the size distribution and refractive index for BC are the same for these models.*

P25, L2-4:

> *This is likely due to a net reduction in BC absorption due to the increase in the assumed density of BC (1.0 g cm^{-3} in GEOS-Chem v9-02, 1.8 g cm^{-3} in GC-RT) that is partially offset by the increased imaginary refractive index for BC in GC-RT.*

21. page 24, line 13: What improvements might this be?

One potential improvement that would reduce both absorption and scattering would be to increase the assumed density of OC to match that used in the other fixed size distribution models. However, this would likely reduce all three wavelengths, not just at 450/470 nm and 550/532 nm. Similarly, the size distribution changes between OPAC and GMI seem to have reduced the scattering more strongly at 700 nm than at 450 or 550 nm. Thus, further investigation and update of the dependence of the complex refractive indices on wavelength might be needed to improve GMI performance.

We have added this discussion to the revised text (P25, L26-31):

> *Increasing the density of OC in GMI to 1.8 g cm^{-3} to match the other fixed-sixe distribution models would likely reduce all three wavelengths equally, and the changes to the fixed size distribution parameters examined here generally*

resulted in stronger absorption and scattering in all wavelengths, so refining the wavelength dependence of the complex refractive indices used in GMI might be the most promising pathway for significant improvements.

Evaluating Model Parameterizations of Submicron Aerosol Scattering and Absorption with In Situ Data from ARCTAS 2008

M. J. Alvarado[1], C. R. Lonsdale[1], H. L. Macintyre[2,*], H. Bian[3,4], M. Chin[4], D. A. Ridley[5], C. L. Heald[5,6], K. L. Thornhill[7], B. E. Anderson[7], M. J. Cubison[8,], J. L. Jimenez[8], Y. Kondo[9], L. K. Sahu[9], J. E. Dibb[10], and C. Wang[2]**

[1]{Atmospheric and Environmental Research, Lexington, Massachusetts, USA}

[2]{Center for Global Change Science, Massachusetts Institute of Technology, Cambridge, Massachusetts, USA}

[3]{Goddard Earth Sciences and Technology Joint Center for Earth Systems Technology, University of Maryland Baltimore County, Baltimore, Maryland, USA}

[4]{NASA Goddard Space Flight Center, Greenbelt, Maryland, USA}

[5]{Department of Civil and Environmental Engineering, Massachusetts Institute of Technology, Cambridge, Massachusetts, USA}

[6]{Department of Earth, Atmospheric and Planetary Science, Massachusetts Institute of Technology, Cambridge, Massachusetts, USA}

[7]{NASA Langley Research Center, Hampton, Virginia, USA}

[8]{Department of Chemistry and Biochemistry, and Cooperative Institute for Research in the Environmental Sciences, University of Colorado, Boulder, Colorado, USA}

[9]{Department of Earth and Planetary Science, University of Tokyo, Tokyo, Japan}

[10]{Department of Earth Sciences and Institute for the Study of Earth, Oceans, and Space, University of New Hampshire, Durham, New Hampshire, USA}

[*]{Now at Public Health England, Chilton, Oxfordshire, UK}

[**]{Now at Tofwerk AG, Thun, Switzerland}

Correspondence to: M. J. Alvarado (malvarad@aer.com)

Abstract

Accurate modeling of the scattering and absorption of ultraviolet and visible radiation by aerosols is essential for accurate simulations of atmospheric chemistry and climate. Closure studies using in situ measurements of aerosol scattering and absorption can be used to evaluate and improve models of aerosol optical properties without interference from model errors in aerosol emissions, transport, chemistry, or deposition rates. Here we evaluate the ability of four externally mixed, fixed size distribution parameterizations used in global models to simulate submicron aerosol scattering and absorption at three wavelengths using in situ data gathered during the 2008 Arctic Research of the Composition of the Troposphere from Aircraft and Satellites (ARCTAS) campaign. The four models are the NASA Global Modeling Initiative (GMI) Combo model, GEOS-Chem v9-02, the baseline configuration of a version of GEOS-Chem with online radiative transfer calculations (called GC-RT), and the Optical Properties of Aerosol and Clouds (OPAC v3.1) package. We also use the ARCTAS data to perform the first evaluation of the ability of the Aerosol Simulation Program (ASP v2.1) to simulate submicron aerosol scattering and absorption when in situ data on the aerosol size distribution is used, and examine the impact of different mixing rules for black carbon (BC) on the results. We find that the GMI model tends to overestimate submicron scattering and absorption at shorter wavelengths by 10-23%, and that GMI has smaller absolute mean biases for submicron absorption than OPAC v3.1, GEOS-Chem v9-02, or GC-RT. However, the changes to the density and refractive index of BC in GC-RT improve the simulation of submicron aerosol absorption at all wavelengths relative to GEOS-Chem v9-02. Adding a variable size distribution, as in ASP v2.1, improves model performance for scattering but not for absorption, likely due to the assumption in ASP v2.1 that BC is present at a constant mass fraction throughout the aerosol size distribution. Using a core-shell mixing rule in ASP overestimates aerosol absorption, especially for the fresh biomass burning aerosol measured in ARCTAS-B, suggesting the need for modeling the time-varying mixing states of aerosols in future versions of ASP.

Matthew Alvarado 5/24/2016 2:53 PM
Deleted: in situ

Matthew Alvarado 5/24/2016 2:53 PM
Deleted: information

Matthew Alvarado 5/24/2016 2:58 PM
Deleted: state

1 Introduction

Atmospheric aerosols can both scatter and absorb ultraviolet and visible (UV-VIS) light, thereby altering the actinic flux and the rates of photolytic reactions in the atmosphere (e.g., Michelangeli et al., 1992; He and Carmichael, 1999). The absorption of UV-VIS light by atmospheric aerosols is dominated by light absorbing carbon (LAC) and mineral dust particles (Bian et al., 2003; Martin et al., 2003). Produced by the incomplete combustion of fossil fuels and biomass, LAC has two major forms: "black carbon" or BC, which is primarily composed of soot; and organic aerosols (OA) that strongly absorb UV-VIS light, called "brown carbon" or BrC (Andreae and Gelencsér, 2006). Both forms of LAC can be internally mixed with or coated by less absorbing, more reflective inorganic and organic species, altering their optical properties (e.g., Liao et al., 1999; Yang and Levy, 2004; Lack and Cappa, 2010).

In situ and regional studies of the impact of LAC aerosols on photolysis rates have found that absorbing aerosols can reduce local photolysis rates and OH concentrations by as much as 40% (Tang et al., 2003; Lefer et al., 2003; Alvarado et al., 2009), substantially reducing the net production rate of O_3 in urban airsheds (Jacobson, 1998; Li et al., 2005) and biomass burning plumes (Tang et al., 2003; Alvarado et al., 2009), with the magnitude of the impact dependent on the concentrations of NO_x and VOCs (He and Charmichael, 1999; Yang and Levy, 2004). Global modeling studies have found similar impacts of LAC on photolysis rates, OH concentrations, and net O_3 production (e.g., Liao et al., 2003). For example, Bian et al. (2003) found that the scattering and absorption of UV-VIS light by aerosols increased global tropospheric mean O_3 by ~1 ppbv and decreased OH by 8%. Martin et al. (2003) found that the light absorption by externally mixed black carbon aerosols decreased the modeled photolysis rate of O_3 to form $O(^1D)$ by a factor of 2 in biomass burning regions and the Ganges Valley, thus decreasing OH concentrations by as much as 40%. Tie et al. (2005) found 10 to 40% reductions in the formation of $O(^1D)$ by photolysis in Europe, eastern Asia, and the Amazon due to externally mixed anthropogenic and biomass burning aerosols. This caused 5 to 40% reductions in HO_x concentrations along with modest changes to O_3 (-4 to +5%).

Furthermore, the scattering and absorption of UV-VIS light by LAC aerosols can lead to a significant climate forcing (the direct effect), but the magnitude of this forcing is uncertain. For example, the review of Bond et al. (2013) estimated the direct radiative forcing (DRF) of atmospheric BC is +0.71 W m^{-2} with 90% uncertainty bounds of (+0.08, +1.27) W m^{-2}.

Chung et al. (2012) used data from the ground based Aerosol Robotic Network (AERONET, Dubovik and King, 2000) to estimate a similar global DRF of 0.65 ± 0.15 W m^{-2} from all LAC aerosols, but in this study brown carbon was estimated to account for ~20% of the total forcing. However, Wang et al. (2014) used the GC-RT model (Heald et al., 2014) combined with AERONET data to obtain a lower DRF estimate of 0.32 W m^{-2} from all LAC aerosols (uncertainty range 0.04 to 0.50 W m^{-2}), with 34% of the forcing coming from BrC. While these uncertainties in the aerosol direct effect are generally smaller than the uncertainties in the forcing due to aerosol-cloud interactions (the indirect effect), they are still a significant cause of differences between climate models.

Accurately accounting for the scattering and absorption of UV-VIS light by LAC aerosols is thus critical for models of atmospheric composition, air quality, and climate change. However, in order to reduce computational expense (so that the saved computational cycles can be used to increase model resolution, number of chemical species, etc.), most global chemical transport models (CTMs), such as the Global Modeling Initiative (GMI) Combo model (Duncan et al., 2007) of the US National Aeronautics and Space Administration (NASA) and GEOS-Chem (Bey et al., 2001), account for this absorption assuming that all aerosol species are externally mixed (i.e., sulfate, sea salt, dust, OA, and black carbon aerosols are not present in the same particle), and that each of these aerosol types have fixed, prescribed size distributions. These simplifications can lead to substantial errors in simulating the impact of LAC aerosols on photochemistry, as these impacts can vary substantially with aerosol size and mixing state. For example, the studies of Liao et al. (1999) and Yang and Levy (2004) showed that internal mixtures of sulfate and BC aerosols can cause larger reductions of photolysis rates than external mixtures. Other theoretical (e.g., Jacobson, 2001) and observational (e.g., Schwarz et al., 2008; Shiraiwa et al., 2010; Lack et al., 2012) studies suggest that coatings on BC aerosol can enhance absorption by 30% or more. For example, Kim et al. (2008) showed that accounting for internally-mixed aerosols and changing aerosol size distributions with time gave a much smaller total negative TOA forcing (−0.12 W m$^{−2}$) of all carbonaceous and sulfate aerosol compounds compared to the cases using one-moment scheme either excluding or including internal mixtures (−0.42 and −0.71 W m$^{−2}$, respectively). However, core-in-shell Mie calculations carried out by Lack and Cappa (2010) suggested that a black carbon particle coated with brown carbon can actually absorb less light than a black carbon particle coated in non-absorbing material, with reductions in absorption of up to 50% relative to clear coatings. In addition, Cappa et al. (2012) found little (~6%)

Matthew Alvarado 5/24/2016 5:30 PM
Deleted: to get

Matthew Alvarado 5/27/2016 7:38 PM
Deleted: reduce

Matthew Alvarado 5/24/2016 3:14 PM
Deleted: intensity

enhancement of BC absorption by coatings in California during the US Department of Energy Carbonaceous Aerosols and Radiative Effects Study (CARES) in June of 2010. However, these observations were made under dry conditions and thus the result may not apply at higher RH.

Thus, while the simplifications used in the global CTMs greatly reduce the computational expense of global studies of the impact of LAC aerosols on photochemistry, it is important to quantify the errors in the simulation of aerosol scattering and absorption that result from the assumption of an external mixture and the chosen size distributions for each aerosol type. In situ closure studies, like the one in this work, allow the accuracy of the aerosol scattering and absorption calculations in these models to be assessed independently of the potential errors in other model processes such as the treatment of aerosol emission, secondary organic aerosol (SOA) formation, and aerosol wet and dry deposition. In these closure studies, ambient measurements of aerosol mass and composition are used as inputs to the aerosol optical property routines of the global models, with the model-calculated aerosol optical properties evaluated using simultaneous in situ measurements of aerosol scattering and absorption. In addition, more detailed aerosol models that allow for time varying size distributions and more complicated internal mixtures of aerosol, such as AER's Aerosol Simulation Program (ASP; Alvarado, 2008; Alvarado and Prinn, 2009; Alvarado et al., 2015) can also be evaluated in these closure studies to help determine if the errors in the global model routines are primarily due to their fixed size distributions, assumptions about external mixtures, their assumptions about the refractive indices of LAC, or interactions between these assumptions.

Matthew Alvarado 5/24/2016 5:33 PM
Deleted: s

Matthew Alvarado 5/24/2016 3:20 PM
Deleted: or

Previous closure studies have looked at both the scattering and absorption of aerosols measured at surface sites (Sciare et al., 2005; Cai et al., 2011), from research vessels (Quinn and Coffman, 1998) and from aircraft (Wex et al., 2002; Cai et al., 2011; Highwood et al., 2012; Esteve et al., 2014). For example, Quinn and Coffman (1998) found agreement in the submicron scattering calculated via a Mie code using the in situ size distribution and composition measurements and measurements from an integrating nephelometer to within measurement uncertainty, but did not get good agreement for supermicron aerosol. More recently, Highwood et al. (2012) used a Mie code to simulate aerosol scattering (450, 550, and 700 nm) and absorption (567 nm) for several aircraft flights during the EUCAARI-LONGREX campaign, finding agreement within the measurement uncertainties of 30%. Esteve et al. (2014) expanded on this work by using a flexible Mie code assuming homogeneous internally mixed spheres. They found that the agreements between the calculation and measurements of absorption and scattering was within measurement uncertainties for EUCAARI-LONGREX, as in Highwood et al. (2012), but that there was poorer agreement for the VOCALS-Rex campaign, where detailed in situ observations of the aerosol size distribution were not available.

In this study, we evaluate four aerosol optical property parameterizations used in global models with in situ data on submicron aerosol scattering and absorption at three wavelengths (450, 550, and 700 nm for scattering, 470, 532, and 660 nm for absorption) gathered during the 2008 Arctic Research of the Composition of the Troposphere from Aircraft and Satellites (ARCTAS) campaign. The four parameterizations evaluated are from the Optical Properties of Aerosol and Clouds (OPAC v3.1; Hess et al., 1998) software package, the GMI Combo model, GEOS-Chem v9-02 (Bey et al., 2001), and the baseline configuration of a version of GEOS-Chem with online radiative transfer calculations (called GC-RT; Heald et al., 2014; Wang et al., 2014). This study differs from the closure studies discussed above in that these aerosol optical property modules, which simulate the aerosol as an external mixture of different components each with mixed size distributions, are evaluated directly without the additional constraints provided by the measured aerosol size distributions. We also use the ARCTAS data to perform the first evaluation of the aerosol optical property calculations in ASP v2.1, and investigate how the use of in situ size distribution information and the use of different mixing rules for BC affects the match with observations.

Matthew Alvarado 5/25/2016 2:22 PM
Deleted:

Section 2 describes the five aerosol optical property models examined in this study, including the ASP v2.1 model, while Section 3 describes the ARCTAS data used. Section 4 summarizes the methodology for the closure studies for both the global models (Section 4.1) and ASP v2.1 (Section 4.2). The results of the global model and ASP closure studies are discussed in Sections 5 and 6, respectively. The conclusions of the study and recommendations for future model development are summarized in Section 7.

2 Aerosol Optical Property Models

2.1 OPAC v3.1

The OPAC package was first described by Hess et al. (1998), and version 3.1 is available online at http://opac.userweb.mwn.de/radaer/opac-des.html#ftp. OPAC v3.1 includes microphysical and optical properties of six types of water clouds, three types of ice clouds and

Matthew Alvarado 5/24/2016 5:34 PM
Formatted: Font:Not Bold

ten aerosol types with size distributions and complex refractive indices chosen to represent typical cases. The optical properties calculated include normalized extinction, scattering, and absorption coefficients, single scattering albedo, asymmetry parameter, and the phase function at 61 wavelengths between 250 nm and 40 µm for up to 8 values of relative humidity. The aerosol components included are "water-insoluble" aerosols (primarily soil particles), water-soluble aerosols (primarily organics and other secondary aerosol components, see Hess et al., 1998), soot, two size modes of sea salt, four size modes of mineral dust, and sulfate droplets. A given aerosol is then modeled as an external mixture of these ten aerosol components. For the aerosol components analyzed in this paper (see Table 1), the optical properties are calculated from the assumed lognormal size distributions and refractive indices using Mie theory.

Matthew Alvarado 5/24/2016 5:33 PM
Deleted: six water clouds, three ice clouds, and 10 aerosol components,

Matthew Alvarado 5/27/2016 7:29 PM
Deleted:

Matthew Alvarado 5/24/2016 5:33 PM
Formatted: Font:Bold

2.2 NASA GMI Combo Model

The NASA GMI Combo model is a modular chemical transport model (Duncan et al., 2007; Strahan et al., 2007; Bian et al., 2009) that includes treatment of both stratospheric and tropospheric processes. Major atmospheric aerosol components included in the model are sulfate, black carbon, OA, dust, and sea-salt using either GOCART (Chin et al., 2002, 2009; Ginoux et al., 2001, 2004) or the University of Michigan/Lawrence Livermore National Laboratory IMPACT model (Liu et al., 2007).

Within the NASA GMI Coupled model, the impact of aerosols on photolysis rates is calculated using the FAST-JX model (v6.5). FAST-JX contains lookup tables of the wavelength dependent extinction efficiencies, single scattering albedos, and phase function coefficients for 14 aerosol types at 4 wavelengths (300, 400, 600, and 1000 nm) and at 7 values for relative humidity (0%, 50%, 70%, 80%, 90%, 95%, and 99%; see Supplement). The 14 aerosol types include OA, black carbon, tropospheric, volcanic, and stratospheric sulfate, two modes of sea salt, and seven modes of mineral dust. The optical properties in these tables are based on Mie theory calculations (Mishchenko et al., 2002; Martin et al., 2003), which were initially performed for GEOS-Chem. The relative humidity dependent complex indices of refraction (calculated using a simple volume-average mixing rule, see Hess et al., 1998) and lognormal size distributions are taken from the Global Aerosol Data Set (GADS) of Köpke et al. (1997), which is in turn based on OPAC v3.1 except that (a) all standard deviations of the modes are set to 2.0 and (b) the dry mode radius of sulfate used in OPAC v3.1 (0.0695 µm) is reduced to 0.05 µm. FAST-JX then interpolates the aerosol

Matthew Alvarado 5/24/2016 5:35 PM
Deleted: the

parameters contained in the look-up tables and calculates the average parameters for external mixtures of the aerosol types.

2.3 GEOS-Chem v9-02

The aerosol optical property parameterizations within GEOS-Chem v9-02 (Bey et al., 2001) follow a similar approach to the NASA GMI model, but the refractive indices and size distributions of several aerosol components have been updated based on the work of Wang et al. (2003a,b), Drury et al. (2010), and Jaegle et al. (2011). Table 1 shows the differences in the lognormal size distribution parameters, densities, and refractive indices for the aerosol types examined in this study from OPAC v3.1, GMI, GEOS-Chem v9-02, and the baseline configuration of GC-RT (discussed below). As in GMI, the optical properties for GEOS-Chem v9-02 are based on Mie theory calculations, but with changes to the assumed size distribution, refractive indices, and densities as noted in Table 1. In general, the geometric standard deviation of the size distribution σ used in GMI was reduced from the values of 2.0 to 1.6 for tropospheric sulfate, OA, and BC, and to 1.5 for the accumulation mode of sea salt. Furthermore, following Drury et al. (2010) the assumed geometric mean radius (r_g) of OA was increased by a factor of 3, the mean radius of BC was doubled, and the mean radius of sulfate was increased from 0.05 µm to 0.07 µm. Following Jaegle et al. (2011), the mean radius of the accumulation mode sea salt was reduced from 0.21 µm to 0.09 µm. The refractive index of tropospheric sulfate was also updated to reflect that of ammonium sulfate, rather than sulfuric acid aerosols.

Matthew Alvarado 11/17/2015 3:28 PM
Deleted: Table 1

2.4 Baseline GC-RT

GC-RT (Heald et al., 2014; Wang et al., 2014) is a configuration of GEOS-Chem that is coupled with the radiative transfer model RRTMG (Iacono et al., 2008) with modified aerosol optical properties relative to the standard GEOS-Chem code. Here we test the aerosol optical properties calculated by the "baseline" configuration of GC-RT described by Wang et al. (2014). As in GMI and GEOS-Chem v9-02, the optical properties in GC-RT are based on Mie theory calculations. The aerosol optical property calculation in the baseline configuration of GC-RT differs from GEOS-Chem v9-02 in that the BC density and refractive index are adjusted to the values recommended by Bond and Bergstrom (2006), which have been found to agree better with observations (Park et al, 2003; Stier et al, 2007; Kondo et al., 2011). These changes are shown in Table 1.

Matthew Alvarado 11/17/2015 3:28 PM
Deleted: Table 1

2.5 ASP v2.1

ASP (Alvarado and Prinn, 2009) simulates the gas-phase, aerosol-phase, and heterogeneous chemistry of young biomass burning smoke plumes, including the formation of O_3 and secondary inorganic and organic aerosol. ASP is a flexible, sectional size-resolved aerosol model that includes modules to calculate aerosol thermodynamics, gas-to-aerosol mass transfer (condensation/evaporation), coagulation of aerosols, and aerosol optical properties. ASP is generally run as a single box model, but it can be implemented as the chemistry subroutine of larger Eulerian and Lagrangian chemical transport models (e.g., Alvarado et al., 2009). ASP has been extensively used to study the chemical and physical transformations of aerosols within biomass burning smoke plumes and the optical properties of aerosols (Alvarado and Prinn, 2009; Alvarado et al., 2015) including the first simultaneous simulations of the fluid dynamics, radiative transfer, gas-phase chemistry, and aerosol-phase chemistry in a young biomass burning smoke plume (Alvarado et al., 2009). However, the aerosol optical property routines of ASP have not been previously evaluated with in situ data.

In this study we are using ASP v2.1 (Alvarado et al., 2015). The modules of ASP v2.1 most relevant to the current study are the modules for aerosol size distribution, thermodynamics, and optical properties. These modules are described in detail below.

2.5.1 ASP Aerosol Size Distribution

Matthew Alvarado 5/24/2016 5:22 PM
Deleted: and Thermodynamics

Aerosols are represented in ASP v2.1 as a single, internally-mixed moving-center sectional size distribution (Jacobson 1997, 2002, 2005). In this representation, size bin boundaries remain fixed while the mean particle size within the bin is allowed to change with time, and all particles in a size bin are assumed to have the same composition (except when the external mixture (EXT) mixing rule is used, see Section 2.5.2). In this study, the aerosol size distributions were modeled at a high resolution by using 40 size bins, 38 logarithmically distributed between diameters of 10 nm and 20 µm and one bin each for particles smaller than 10 nm or larger than 20 µm. Our tests found that increasing the number of bins used in ASP v2.1 to 100 changed the calculated optical properties by only ~1%. In ASP v2.1, the mass fractions of different aerosol components are assumed to be independent of aerosol size, so the relative aerosol composition is the same in each size bin. This assumption is likely to be violated for aerosols that contain significant amounts of BC (see Section 6.2), and is planned to be relaxed in future model development.

Matthew Alvarado 5/24/2016 5:37 PM
Formatted: Font:Not Bold, English (US)

Matthew Alvarado 5/24/2016 5:37 PM
Deleted: each particle in a size bin is assumed to have the same composition

Matthew Alvarado 5/24/2016 5:44 PM
Formatted: Font:Not Bold, English (US)

Matthew Alvarado 5/24/2016 5:43 PM
Deleted: and two bins for particles smaller than 10 nm or larger than 20 µm

2.5.2 ASP Aerosol Optical Properties

As part of this work, we have extensively updated the calculations of aerosol optical properties within ASP v2.1 beyond those described by Alvarado (2008) and Alvarado and Prinn (2009). We have implemented spectrally-varying complex refractive indices for wavelengths between 250-700 nm for five aerosol components (H_2O, soot, sulfate, sea salt, and OA) based on those from OPAC v3.1 (Hess et al., 1998; see also Section 2.1 above). Similar to the procedure used in the NASA GMI Combo model and GEOS-Chem, we assume (1) that organics follow the OPAC v3.1 refractive indices of so-called "water-soluble particulate matter", (2) that all sulfate and nitrate salts follow the OPAC sulfate indices, (3) that all chloride salts follow the OPAC sea salt indices, and (4) that all BC follows the OPAC soot indices. The real refractive index of the inorganic aqueous solution (if present) is calculated using the molar refraction approach of Tang (1997) and Tang et al. (1997).

As in Alvarado and Prinn (2009), we assume here that all particles are spherical for the purposes of calculating their optical properties. ASP v2.1 has also been updated to include four mixing rules for the refractive indices of black carbon and the other aerosol components: (1) a volume-average (VA) dielectric constant mixing rule for all aerosol components; (2) a core-shell (CS) mixing rule, where a spherical core of BC is surrounded by a spherical shell of all other aerosol components (with the refractive index of the shell calculated using the volume-average dielectric constant mixing rule); (3) the Maxwell Garnett (MG) mixing rule, which here assumes that BC is present as a single randomly distributed inclusion within the particle (Maxwell Garnett, 1904); and (4) an external mixture (EXT) of BC and the other aerosols components, with both sets of particles having the same size distributions but with the relative number of particles determined by the relative volume concentrations. Mie calculations of aerosol optical properties for each bin of the size distribution are performed within ASP using the publicly available program DMiLay, which is based on the work of Toon and Ackerman (1981).

3 ARCTAS Data

The objective of the NASA ARCTAS campaign (Jacob et al., 2010) conducted in April and June-July 2008 was to better understand the factors driving current changes in Arctic atmospheric composition and climate. It used chemical and radiative measurements from three research aircraft (DC-8, P-3, B-200) to interpret and augment the continuous observations of Arctic atmospheric composition from satellites. The aircraft were based in

Matthew Alvarado 5/24/2016 2:47 PM

Deleted: The inorganic thermodynamics module in ASP v2.1 includes H_2O, NH_3, the acids HNO_3, HCl, and H_2SO_4, the ions H^+, NH_4^+, Na^+, K^+, Ca^{2+}, Mg^{2+}, SO_4^{2-}, HSO_4^-, NO_3^-, Cl^-, OH^-, and their various salts (Alvarado and Prinn, 2009; Alvarado, 2008). Binary and mixed activity coefficients for the various ion pairs are calculated using the Kusik-Meissner approach (Kusik and Meissner, 1978) when binary coefficient data are available; otherwise they are constructed using an appropriate combination of the available binary activity coefficients, as in Kim et al. (1993a) and Steele (2004). Equilibrium constants for electrolyte and gas-particle equilibrium reactions, as well as the deliquescence relative humidities (DRHs) of the electrolytes have been updated to match ISORROPIA II (Fountoukis and Nenes, 2007). The water associated with the inorganic aerosol is calculated via an iterative solution based on the Gibbs-Duhem equation (Steele, 2004; Alvarado, 2008). Equilibrium concentrations of the gas and aerosol species are then calculated using the Mass Flux Iteration (MFI) approach of Jacobson (2005). This approach to inorganic aerosol thermodynamics compares well with other inorganic aerosol thermodynamics models such as ISORROPIA (Nenes et al., 1998; Fountoukis and Nenes, 2007), as shown by Steele (2004) and Alvarado (2008). ... [1]

Matthew Alvarado 5/25/2016 9:29 AM

Deleted: in

Matthew Alvarado 5/25/2016 9:30 AM

Deleted: s

Alaska in April (ARCTAS-A) and in western Canada in June-July (ARCTAS-B). The focus of ARCTAS-A was to examine the long-range transport of anthropogenic pollution to the Arctic, while ARCTAS-B was more focused on the impacts of boreal forest fires on regional and global atmospheric composition. The summer ARCTAS-B deployment was preceded by one week of flights over California sponsored by the California Air Resources Board (CARB) to address regional issues of air quality and climate forcing.

Here we use data from the DC-8 aircraft during all three phases of ARCTAS, as described in detail below, to evaluate the aerosol optical property models. All analyses in this study used the "merged" data set averaged to the 10s time resolution of the Ultra-High Sensitivity Aerosol Spectrometer (UHSAS).

3.1 Aerosol Mass Concentrations and Composition

On the NASA DC8, submicron black carbon mass was measured with the University of Tokyo Single Particle Soot Photometer (SP2; Moteki and Kondo, 2007, 2008). The SP2 measures BC volume for particles with volume equivalent diameters between 90 nm and 1.0 µm. The measured BC volume is then converted to BC mass using an assumed density of 1.8 g/cm^3. The uncertainty in the BC mass measurements is ±30%. As a rough estimate, we calculate that by not measuring the BC mass below 90 nm, using the measured SP2 mass could bias a perfect absorption model low in absorption by about ~10%. However, as shown in Section 5 and 6, most models studied here overestimate submicron aerosol absorption, so this potential bias would tend to move the models closer to the observations. In addition, this bias is smaller than the potential bias in the absorption measurements due to the filter corrections, as noted in Section 3.3.

An Aerodyne high-resolution, time-of-flight aerosol mass spectrometer operated by the University of Colorado, Boulder (HR-ToF-AMS, hereafter AMS; DeCarlo et al., 2008; Cubison et al., 2011) was used to measure ammonium, chloride, nitrate, sulfate, and organic aerosol mass concentrations. The AMS primarily samples submicron aerosols, with 0% transmission for vacuum aerodynamic diameters below 35 nm and an approximate PM_1 size cut in vacuum aerodynamic diameter (DeCarlo et al., 2004; Canagaratna et al., 2007). The uncertainty of the AMS mass concentrations measurements (2σ) is ±34% for the inorganics and ±38% for the organics (Bahreini et al., 2009; Cubison et al., 2011), dominated by the uncertainty in the particle collection efficiency due to particle bounce (e.g., Huffman et al., 2005).

In addition, data on the concentration of water-soluble organic carbon (WSOC) in submicron aerosol is provided by the Particle In Liquid Sampler (PILS-WSOC) of the Georgia Institute of Technology (Sullivan et al., 2006), with an uncertainty of ±45%. The measured WSOC was converted to total organic mass using a factor of 1.6. This value is uncertain to at least ±0.4, but as our total OA concentration is determined by the AMS and the relative humidites of the optical property measurements were low, this assumption has little impact on our results. The PILS-WSOC data is used in the ASP closure study to separate water-soluble and water-insoluble organic aerosol (see Section 4.2 below).

The AMS data were also supplemented with measurements of additional inorganic cations from the University of New Hampshire Soluble Acidic Gases and Aerosol (UNH SAGA, Dibb et al., 2003) instrument. SAGA collects non-size selected (“bulk”), isokinetically-sampled aerosols onto a teflon filter. The ions are then extracted off the filter with deionized water and analyzed via ion chromatography. In addition to the ions measured by the AMS, SAGA provides measurements of the refractory cations sodium (±0.1 ug/m^3 at 1013 hPa and 273.15 K), potassium (±0.017 ug/m^3), magnesium (±0.011 ug/m^3), and calcium (±0.018 ug/m^3). In order to convert the SAGA bulk measurements of these ions into submicron concentrations consistent with the AMS time-resolution, we use the bulk SAGA data to determine a bulk ratio of these refractory cations to aerosol sulfate, and to combine these ratios with the AMS measured sulfate concentrations to estimate the submicron mass concentrations of the refractory cations.

To test this procedure, we compare AMS measured submicron nitrate, ammonium, and chloride mass concentrations versus the concentrations estimated with the above SAGA-based procedure. The match is very good for nitrate and ammonium (not shown), but submicron chloride (not shown) is larger by the SAGA based procedure, as expected since SAGA is sensitive to refractory chlorides such as NaCl and the AMS is not. However, as we expect the aerosol in the ARCTAS campaign to be dominated by the species measured by the AMS and the SP2, errors in our estimates of the submicron refractory cation mass should have little impact on our closure study results.

Matthew Alvarado 5/25/2016 3:55 PM
Deleted: OA and BC aerosols

Matthew Alvarado 5/25/2016 3:55 PM
Deleted: this

3.2 Aerosol Size Distribution

In this study, we use the in situ measurements of dry aerosol size distribution provided by the instruments of the NASA Langley Aerosol Research Group (LARGE; Anderson et al., 1998). Specifically, we use the dry aerosol size distribution data from the TSI Scanning Mobility Particle Sizer (SMPS), the Droplet Measurement Technologies (DMT) Ultra-High Sensitivity Aerosol Spectrometer (UHSAS), and the TSI Aerodynamic Particle Sizer (APS) Model 3321.

The UHSAS is our primary source of size distribution information as the size range measured by the UHSAS (optical particle diameters between 60 nm to 1000 nm) measures the particles most likely to affect optical properties in the UV-VIS. The UHSAS has 99 bins geometrically distributed in this size range, and gathers data every 10 s. The estimated precision of the UHSAS is 5% in the particle size, and 20% in the particle number concentrations in each bin. Note that, as the UHSAS is an optical instrument, it can give incorrect size information if the refractive index of the particles is far from that of the polystyrene latex spheres used for calibration. This artifact can lead to a small underestimate of the size of submicron particles when it is not taken into account, thereby leading to an underestimate of scattering (e.g., Kassianov et al., 2015). However, we expect that this effect on our study will be small relative to the stated precision of the UHSAS.

The TSI SMPS measures dry aerosol size distributions in 54 size bins with geometric diameters between 8.8 nm and 399.7 nm. The time resolution is lower than the UHSAS (105s for the SMPS versus 10 s for the UHSAS), and so care has to be taken in matching SMPS size distributions with the UHSAS, as described in Section 4.2. The estimated precision of the SMPS is 5% in the particle size, and 25% in the particle number concentrations in each bin.

Matthew Alvarado 5/24/2016 5:52 PM
Deleted: s

The TSI APS measures dry aerosol size distributions in 13 size bins with aerodynamic diameters between 0.583 μm and 7.75 μm. The time resolution is the same as the UHSAS, but the measured diameters are different (optical diameter for the UHSAS, aerodynamic diameter for the APS). Converting continuum-regime aerodynamic diameter D_{aero} to geometric diameter D_{geo} is done through the equation:

Matthew Alvarado 5/24/2016 5:53 PM
Deleted: n

$$D_{geo} = D_{aero}\sqrt{\frac{X}{\rho}}. \qquad (3)$$

where ρ is the particle density and X is the "dynamic shape factor" that accounts for the non-sphericity of the particles (for spheres, $X = 1.0$, otherwise $X > 1$). The estimated precision of the APS is 10% in the particle size, and 20% in the particle number concentrations in each bin.

3.3 Aerosol Optical Properties

In this study, we use the in situ measurements of dry aerosol scattering and absorption provided by the LARGE suite of instruments. During ARCTAS, LARGE measured dry total aerosol scattering and hemispherical backscattering coefficients at three wavelengths (450 nm, 550 nm, and 700 nm) using a TSI model 3563 nephelometer with an estimated precision of 0.5 Mm^{-1}. These total scattering coefficients were then corrected for truncation errors using the procedure described by Anderson and Ogren (1998), who report a measurement reproducibility of ±1%. Thus the actual uncertainty in the scattering meaurements is ±1% or ±0.5 Mm^{-1}, whichever is larger. A Radiance Research (RR) nephelometer with a 1 μm cut cyclone measured the scattering of submicron aerosols at 532 nm. This data allowed an estimate of the submicron scattering at 450nm, 550 nm, and 700 nm by comparison of the two nephelometers when they were sampling mainly submicron particles (i.e., a fine mode fraction > 0.6).

Dry total and submicron absorption was also measured at three wavelengths (467 nm, 532 nm, and 660 nm) using a RR Particle Soot Absorption Photometer (PSAP) with an estimated precision of 0.2 Mm^{-1}. These filter-based absorption measurements were corrected to in situ values using two methods: one from Virkkula (2010) and one from Lack et al. (2008). These two corrections can differ by about 20-30%, with Virkkula (2010) giving lower aerosol absorption. Thus the practical uncertainty in the absorption measurement is estimated as at least 20-30%. Most of our analysis is based on the correction of Lack et al. (2008), but we discuss the sensitivity of our conclusions to the choice of correction as well. The PSAP submicron absorption measurement is well correlated with the submicron BC mass (not shown), with an overall r^2 of 0.64, but the data is uncorrelated for low BC mass concentrations (<0.03 μg m^{-3}), which occurs for 261 out of 10,356 data points in our absorption analysis. However, as we have no clear evidence that these PSAP data points are incorrect and excluding them does not appreciably change the conclusions of our study, we have included these data points in our analysis below.

Matthew Alvarado 5/25/2016 3:18 PM
Formatted: English (US), Not Highlight

Matthew Alvarado 5/27/2016 7:26 PM
Formatted: English (US)

Matthew Alvarado 5/27/2016 7:26 PM
Formatted: English (US)

Matthew Alvarado 5/27/2016 7:26 PM
Formatted: English (US)

4 Closure Study Methodology

4.1 Fixed Size Distribution Parameterizations

As OPAC, GMI, GEOS-Chem, and GC-RT all share a common heritage and features (i.e., external mixtures of fixed size distributions of the various aerosol components) our closure study methodology for all four parameterizations is also similar. The general procedure is shown in Figure 1a. The first step is to assign the measured aerosol mass concentrations to the different aerosol types. In this study we focus on tropospheric, submicron aerosol, as detailed composition data is available from the AMS and SP2 for this size range, and thus we exclude the mineral dust, stratospheric sulfate, volcanic sulfate, and coarse mode sea salt aerosol types. The SP2-measured submicron mass of BC is assigned to the BC (for GMI, GEOS-Chem, and GC-RT) or SOOT (for OPAC) aerosol types. The AMS-measured submicron OA mass is assigned to the OA (for GMI, GEOS-Chem, and GC-RT) or WASO (for OPAC) aerosol types. For the inorganic species measured by the AMS and SAGA, we calculate “equivalent electrolytes” consistent with the measured and estimated submicron ion concentrations (see Equation 17.72 of Jacobson, 2005). The sulfate- and nitrate-containing electrolytes are then assigned to the tropospheric sulfate (for GMI, GEOS-Chem, and GC-RT) and SUSO (for OPAC) aerosol types, while the chloride-containing electrolytes are assigned to the accumulation mode sea salt type.

Matthew Alvarado 11/17/2015 3:28 PM
Deleted: Figure 1

The second step involves determining the submicron scattering coefficient, absorption coefficient, single scattering albedo (SSA), and asymmetry parameter for each aerosol type at the measured wavelengths and relative humidities (RHs). This is done through linear interpolation of the values present in the look-up tables for each aerosol parameterization. As the LARGE instruments measure dry optical properties, the RH used in the interpolation should not be the ambient RH, but instead is the RH in the inlet prior to the measurement. Here, we used the measured inlet RH in all comparisons. This “dry” RH is generally near 0%, but can get as high as 20%.

For GMI, GEOS-Chem, and GC-RT, the tabulated properties include the extinction efficiency (Q_{ext}), effective radius (r_{eff}), and SSA (ω) for each aerosol type j. After correction for wavelength and RH as described above, the volume extinction coefficent ($k_{ext,j}$) for each aerosol type is calculated from these properties by the equation:

$$k_{ext,j} = \frac{3}{4}\frac{Q_{ext,j}}{r_{eff,j}}\frac{m_j}{\rho_j}. \qquad (4)$$

where m_j is the mass concentration for each aerosol type (μg/m^3, corrected to ambient temperature and pressure) and ρ_j is the particle density. The scattering and absorption coefficients are then calculated as $k_{scat,j} = \omega_j k_{ext,j}$ and $k_{abs,j} = (1-\omega_j)k_{ext,j}$. The k_{ext}, k_{scat}, k_{abs}, and ω for each aerosol type are then combined together to give the model estimate of the optical properties for the submicron aerosol mixture. For k_{ext}, k_{scat}, and k_{abs} this is a simple sum, e.g. $k_{scat} = \sum_j k_{scat,j}$, and ω is the ratio of k_{scat} to k_{ext}.

For OPAC, the tabulated properties include values of $k_{ext,j}$, $k_{scat,j}$, $k_{abs,j}$, and ω_j, with $k_{ext,j}$, $k_{scat,j}$, and $k_{abs,j}$ normalized to an assumed particle number concentration of 1 cm^{-3}. These normalized values are multiplied by the ratio of the measured mass concentration m_j to the assumed mass concentration for 1 particle cm^{-3} for each aerosol type. These properties are then corrected for wavelength and RH and combined together as described above for the GMI and GEOS-Chem parameterizations.

4.2 ASP v2.1

The ASP v2.1 model closure studies (see Figure 1b) differ from the other closure studies mainly in the use of the data on the in situ dry aerosol size distribution from the LARGE instrument suite. As noted in Section 3.2 above, this data comes from three different instruments (the SMPS, UHSAS, and APS) with different time resolutions and measuring techniques. Thus combining these observations into a consistent picture of the size distribution is not a straightforward task. Our approach uses the UHSAS observations as the core of our size distribution estimate, as the submicron aerosol optical properties of interest here are likely most sensitive to aerosol within the size range of the UHSAS (60 nm – 1000 nm). We start by creating a "combined" size distribution with the same size resolution as the UHSAS observations, but with an expanded range (i.e., 246 bins with optical diameters between 8.8 nm and 10 μm). For size bins with diameters between 60 nm and 850 nm, the UHSAS data is used directly. For size bins below 60 nm, SMPS data (interpolated to the UHSAS size resolution) is used. As the SMPS has a lower time resolution than the UHSAS, we scale the SMPS data to match the UHSAS data in the size range 60 nm to 100 nm – the scale factor is the slope of the linear regression of the (interpolated) SMPS and UHSAS data

Matthew Alvarado 11/17/2015 3:28 PM
Deleted: Figure 1

in this size range. For size bins larger than 850 nm, the size distribution is based on the APS data, with the conversion factor between aerodynamic and geometric diameter assumed to be 0.8. This value is consistent with the density and shape factors of urban aerosols and solid ammonium sulfate (Reid et al., 2006), and for a spherical particle is equivalent to a density of 1.56 g cm^{-3}. The corrected APS data is used to define a power law that describes how the size distribution decays at optical diameters larger than 850 nm, and this power law is used to extrapolate the UHSAS data for diameters larger than 850 nm.

While ASP v2.1 represented the aerosol as a sectional size distribution as described in Section 2.5.1, the initialization routines of ASP v2.1 require that the dry aerosol size distributions be input as a sum of lognormal modes which are then used to populate the size bins. Thus the “combined” size distribution described above is fit to three lognormal modes (see Equations 13.18 and 13.20 from Jacobson, 2005). The fitting boundaries for the three modes are fixed at 8 – 80 nm, 80 – 400 nm, and 400 nm – 10 µm, as these boundaries coincide with minima in the ARCTAS size distribution data.

Matthew Alvarado 5/25/2016 11:44 AM
Deleted: As

Matthew Alvarado 5/25/2016 11:44 AM
Deleted: s

Matthew Alvarado 5/25/2016 11:44 AM
Deleted: ,

The submicron aerosol mass concentrations of BC, OA, and equivalent electrolytes were calculated as described in Section 4.1. OA was assumed to be fairly involatile and was assigned to the species CBIO (if water-soluble) and POA1 (if not water soluble; Alvarado, 2008). These mass concentrations define the relative mass composition (i.e. mass fractions) in the ASP modes. This aerosol composition was assumed to be the same for all three modes input to ASP v2.1 – while the AMS can be used to obtain size-resolved composition, the averaging times required for this data are large (about an hour), and thus are not useful for comparison to the 10 s resolution optical property data. This implicitly assumes that the size distributions of all aerosol components (BC, OC, and electrolytes) are the same, which may not have been true in the ambient atmosphere.

Matthew Alvarado 5/24/2016 5:30 PM
Deleted: to get

We then used ASP v2.1 to calculate total and submicron k_{scat}, k_{abs}, and ω for wavelengths between 250 nm and 700 nm (at 1 nm resolution) using each of the four mixing rules described above: volume-averaged, core-shell, Maxwell-Garnett, and external mixture. These were compared with the in situ measurements of optical properties from the LARGE instruments.

5 Fixed Size Distribution Parameterization Results

5.1 Scattering

Figure 2 shows a scatterplot of the measured submicron scattering coefficient at 550 nm versus the value calculated using the optical property tables of the GMI Combo model. The slope and correlation coefficient (r^2) of a linear fit to the data from the entire ARCTAS campaign are used in evaluating the models; these values are summarized in Table 2. We see that all four parameterizations explain 70-74% of the variability (e.g., r^2 = 0.70-0.74) in the observed submicron scattering at all three wavelengths, except for the GMI model at 700 nm, where only 58% of the variability is explained. The slopes of the linear fits are between 0.89 and 1.08 for the 450 and 550 nm channels, but the 700 nm channel shows more variability, with a slope of 1.19 for OPAC v3.1 and the slopes for the other models between 0.63-0.68.

Matthew Alvarado 11/17/2015 3:28 PM
Deleted: Figure 2

Matthew Alvarado 11/17/2015 3:28 PM
Deleted: Table 2

However, Figure 2 shows that there can be substantial differences in the results for the different phases of the ARCTAS campaign. The parameterizations generally work best for the ARCTAS-B campaign, which sampled several fresh biomass-burning plumes and thus likely had more externally mixed aerosol samples than the other two phases that sampled more aged pollution. For ARCTAS-B the r^2 values were ~0.75, with slopes between 0.99 and 1.15. In contrast, the models generally overestimate the relatively smaller scattering coefficients of the aged arctic pollution sampled during the ARCTAS-A campaign, with r^2 values of ~0.63 and slopes between 1.5 (OPAC v3.1) and 2.0 (GEOS-Chem v9-02). The ARCTAS-CARB phase shows a clear bifurcation, with some samples overestimated by a factor of 2 or more and some underestimated by similar factors, suggesting two distinct types of aerosols were sampled in this phase. This leads to poor r^2 values for this phase (0.25-0.39) and, as the largest values are generally underestimated, slopes between 0.40 (OPAC v3.1) and 0.70 (GEOS-Chem v9-02).

Matthew Alvarado 11/17/2015 3:28 PM
Deleted: Figure 2

We also examined the distribution of the errors (modeled value – measured value) of the submicron scattering coefficient, as shown in Figure 3 for 550 nm and the GMI model. To reduce the impact of the large dynamic range of the measured scattering coefficients on our analysis, we examined the errors in the logarithm (base 10) of the scattering coefficients, which is equivalent to the logarithm of the ratio of the modeled to measured value. The mean (μ) and standard deviation (σ) of these error distributions are also summarized in Table 2. We prefer these metrics over mean normalized bias (MNB), as with the logarithmic (geometric)

Matthew Alvarado 11/17/2015 3:28 PM
Deleted: Figure 3

Matthew Alvarado 11/17/2015 3:28 PM
Deleted: Table 2

approach an overestimate of a factor of 2 and an underestimate of a factor of 2 average out to no mean error, while the MNB of these two observations would be 25% due to the asymmetry of overestimates and underestimates when expressed as percentages. However, the use of MNB instead of μ does not substantially alter the conclusions of our study, and values for MNB are also discussed below.

The spread of the errors is very similar for all models and wavelengths, with σ of ~0.25, which is equivalent to a standard deviation of a factor of 1.8 about the mean. The histograms of the errors show little skew to either side of the mean value. The models give a positive bias at 450 and 550 nm (see Table 2), with the GMI model having the lowest mean bias in these channels (μ = 0.06 and 0.09, respectively, equivalent to a geometric mean overestimate of 15% and 23%, and an MNB of 35% and 46%). As the 450 nm channel is closest to the UV wavelengths important in photolysis, we would thus expect the GMI model to perform best in modeling the impact of aerosols on photolysis rates. GEOS-Chem v9-02 has a slightly smaller negative bias (-0.04, equivalent to a geometric mean underestimate of 9% and an MNB of 8.5%) than GMI (μ = -0.05, geometric mean underestimate of 11%, MNB of 16%) in the 700 nm channel. The results for GC-RT are similar to GEOS-Chem v9-02 at 450 and 550 nm, but the negative bias at 700 nm is about twice as large on average in GC-RT as it is in GMI or GEOS-Chem v9-02.

In order to interpret these closure study results, it is useful to estimate the values of μ and σ we would expect from a perfect model based on the uncertainty in the input mass concentrations and the uncertainty in the scattering measurement. Taking the sum of the squares in the relative standard errors in the mass concentrations of OA (19%), sulfate (17%), nitrate (17%), ammonium (17%), chloride (17%), and BC (30%), as well as the estimated nephelometer uncertainty (1%) gives an overall uncertainty estimate of ±49%, corresponding to a σ of 0.17. Thus even a perfect model would have a fairly significant spread in it's histogram of errors. However, as we are using ~10,000 data points in our comparison, the expected error in μ is about a factor of 100 lower, and thus we would expect $|\mu| \ll 0.01$.

5.2 Absorption and SSA

Figure 4 shows a scatterplot of the measured submicron absorption coefficient at 532 nm versus the value calculated using the optical property tables of the GMI model. The PSAP measurements have been corrected using the approaches of Lack et al. (2008) (Figure 4a) and

Matthew Alvarado 5/27/2016 7:16 PM
Formatted: Font:Not Italic, English (US)

Matthew Alvarado 5/27/2016 7:16 PM
Formatted: English (US)

Matthew Alvarado 5/27/2016 7:16 PM
Formatted: Font:Not Italic, English (US)

Matthew Alvarado 5/27/2016 7:16 PM
Formatted: English (US)

Matthew Alvarado 5/27/2016 7:16 PM
Formatted: Font:Not Italic, English (US)

Matthew Alvarado 5/27/2016 7:16 PM
Formatted: English (US)

Matthew Alvarado 5/27/2016 7:16 PM
Formatted: English (US)

Matthew Alvarado 5/27/2016 7:16 PM
Formatted: Font:Not Italic, English (US)

Matthew Alvarado 11/17/2015 3:28 PM
Deleted: Figure 4

Matthew Alvarado 5/24/2016 5:55 PM
Deleted: the shows

Matthew Alvarado 11/17/2015 3:28 PM
Deleted: Figure 4

Virkkula (2010) (Figure 4b). As stated in Section 3.3 above, the Virkkula (2010) correction generally gives 20-30% lower aerosol absorption coefficients than the Lack et al. (2008) correction. As the models tended to overestimate aerosol absorption using both corrections, we discuss our results relative to the Lack et al. (2008) corrected values. Results for all model-wavelength combinations using the Lack et al. (2008) correction are summarized in Table 3. Unlike for scattering, the absorption coefficient slopes and correlations are fairly consistent between the ARCTAS-B and ARCTAS-CARB phases of the campaign, but the ARCTAS-A phase shows larger model overestimates of aerosol absorption for the aged Arctic pollution sampled in that campaign. The global model parameterizations can explain 65-72% of the observed variability, comparable to but a little worse than their performance for scattering (see Section 5.1), with slopes between 0.75 (GMI, 660 nm) and 1.21 (GEOS-Chem v9-02, 532 nm).

Figure 5 shows the histogram of the errors in the logarithm of the submicron aerosol absorption coefficient for GMI at 532 nm, while the mean and standard deviation for all model-measurement combinations are summarized in Table 3. The expected values of μ and σ from a perfect model are $\ll 0.01$ and ~0.20, respectively, reflecting the input uncertainties discussed for scattering in Section 5.1 as well as the ~30% uncertainty in converting the filter-based PSAP measurement to the ambient absorption. The spread of the errors (measured by the standard deviation σ) is between 0.24-0.29 for all model-wavelength combinations, giving a standard error of a factor of ~1.7 to 2.0 around the mean bias. We can see that while all the models show a positive mean bias for aerosol absorption at all wavelengths, the GMI model has the smallest mean bias at all wavelengths, with a maximum bias at 532 nm ($\mu = 0.06$, or a 15% geometric mean overestimate, and an MNB of 39%). Similar results hold when the Virkkula (2010) correction is used, but the geometric mean overestimate for GMI at 532 nm increases to 55%. Thus while we can conclude the GMI parameterization performs the best for submicron aerosol absorption of the global model parameterizations evaluated in this study, we can only conclude that its geometric mean error is within the range of 0-55%, depending on wavelength and PSAP correction. Table 3 also shows that the mean overestimate in aerosol absorption in GEOS-Chem v9-02 has been substantially reduced, but not eliminated, by the improved values for BC density and refractive index in GC-RT (e.g., from $\mu = 0.27$ and MNB of 120% in GEOS-Chem v9-02 to $\mu = 0.22$ and MNB of 95% in GC-RT at 532 nm), and the correlation coefficients are slightly improved as well.

Matthew Alvarado 11/17/2015 3:28 PM
Deleted: Figure 4

Matthew Alvarado 11/17/2015 3:28 PM
Deleted: Table 3

Matthew Alvarado 11/17/2015 3:28 PM
Deleted: Figure 5

Matthew Alvarado 11/17/2015 3:28 PM
Deleted: Table 3

Matthew Alvarado 5/27/2016 7:17 PM
Formatted: Font:Not Italic

Matthew Alvarado 11/17/2015 3:28 PM
Deleted: Table 3

Matthew Alvarado 5/27/2016 7:17 PM
Formatted: Font:Italic

Figure 6 shows the results for Single Scattering Albedo (SSA) for the GMI model at 550 nm. The Lack et al. (2008) measured absorptions at 532 nm and 660 nm were used to derive an absorption Angstrom exponent that was then used to estimate the observed absorption at 550 nm. As expected, since both the GMI scattering and absorption comparisons showed small positive biases at this wavelength (see Tables 2 and 3), the GMI calculation of SSA is relatively unbiased, as shown in Table 4. However, the spread of the errors is large (σ= 0.05), and the correlation between the modeled and measured values is poor (r^2 = 0.06). Note that the size of the uncertainties in SSA seen in Table 4 can have a significant impact on estimates of global aerosol DRF. For example, Loeb and Su (2010) found that a SSA perturbation of 0.03 over land and 0.06 over ocean could lead to errors in all-sky DRF of -0.73 to +1.11 W m^{-2}.

We explored whether averaging the observations at 1 and 5 minute intervals would reduce the spread in the SSA errors and improve the correlation. However, the spread of errors only decreased to σ =0.03 when the data is averaged to 5 minute intervals, and the correlation coefficient only increased to r^2 = 0.22. Thus, while the GMI model gives reasonable mean values for SSA, the calculated value tends to be significantly wrong for any given data point. In addition, the GEOS-Chem v9-02 and GC-RT SSA predictions show similar biases and spread of errors, with GC-RT performing slightly better than the other models at 450 nm.

6 ASP v2.1 Results

6.1 Impact of Size Distribution Data on Aerosol Scattering

As expected, when ASP v2.1 is given aerosol size distribution data from the LARGE instrument suite, it does a substantially better job of modeling the observed aerosol scattering than the global model parameterizations discussed in Section 5.1. Figure 7 shows the scatterplot and histogram of the errors in submicron aerosol scattering for ASP v2.1 at 550 nm. The results for a core-shell (CS) BC mixing rule are shown, but the results for all other mixing rules are similar, as shown in Table 5. Note that there are far fewer data points in Figure 7a than in Figure 2 for the GMI model (1,771 versus 10,629). This is because the ASP v2.1 closure requires all three LARGE size distribution instruments to be working at the same time as the AMS, SP2, and other composition instruments, which reduces the amount of available data. With the size distribution data, ASP v2.1 with the core-shell mixing rule is able to explain 88-89% of the observed variability in aerosol scattering, with linear regression

Matthew Alvarado 11/17/2015 3:28 PM
Deleted: Figure 6

Matthew Alvarado 5/27/2016 9:18 PM
Formatted: English (US)

Unknown
Field Code Changed

Matthew Alvarado 11/17/2015 3:28 PM
Deleted: Table 4

Matthew Alvarado 5/27/2016 9:18 PM
Formatted: English (US)

Matthew Alvarado 5/27/2016 9:18 PM
Formatted: Font:Not Bold, English (US)

Matthew Alvarado 5/27/2016 9:18 PM
Formatted: English (US)

Matthew Alvarado 11/17/2015 3:28 PM
Deleted: Figure 7

Matthew Alvarado 5/24/2016 3:00 PM
Deleted: state

Matthew Alvarado 5/24/2016 3:00 PM
Deleted: states

Matthew Alvarado 11/17/2015 3:28 PM
Deleted: Table 5

Matthew Alvarado 11/17/2015 3:28 PM
Deleted: Figure 7

Matthew Alvarado 11/17/2015 3:28 PM
Deleted: Figure 2

Matthew Alvarado 5/24/2016 3:05 PM
Deleted: state

slopes of 0.99, 1.00, and 1.07 at 450, 550, and 700 nm, respectively. The maximum mean (logarithmic) bias is $\mu = -0.03$ (equivalent to a mean underestimate of 7%), and the standard deviation of the logarithmic errors (σ) is only 0.17, equivalent to a factor of 1.5. Given that the size distribution data is itself uncertain to 20% before the instruments are stitched together, this is remarkably good model performance - we estimate that a perfect model would have a σ of 0.13 due to the uncertainty in the size distributions and the relative mass contributions. Together this implies that ASP v2.1 is able to model more than 90% of the scattering data points to within a factor of 2.

Matthew Alvarado 5/27/2016 7:18 PM
Formatted: Font:Not Italic

Matthew Alvarado 5/27/2016 7:18 PM
Formatted: Font:Not Italic

6.2 Impact of Size Distribution Data and Black Carbon Mixing Rule on Aerosol Absorption

Matthew Alvarado 5/24/2016 3:05 PM
Deleted: State

In contrast to the results for scattering, ASP v2.1, with aerosol size distribution data from the LARGE instrument suite, has difficulty reproducing the observations for aerosol absorption. Figure 8a shows a scatterplot of the measured submicron absorption coefficient versus the value calculated by ASP v2.1 using a CS mixing rule. While overall slope (0.93 ± 0.12) is reasonable, there are clear problems in the simulation of the absorption observations from ARCTAS-B and CARB, leading to a poorer correlation coefficient ($r^2 = 0.44$) and a larger spread in the errors ($\sigma = 0.32$, see Figure 8b) than was seen for the global parameterizations using fixed size distributions and external mixtures. We estimate that a perfect model would have a σ of 0.17 due to the uncertainty in the size distributions, the relative mass contributions, and in the absorption measurement.

Matthew Alvarado 11/17/2015 3:28 PM
Deleted: Figure 8

Matthew Alvarado 5/24/2016 3:05 PM
Deleted: state

Matthew Alvarado 11/17/2015 3:28 PM
Deleted: Figure 8

Matthew Alvarado 5/27/2016 7:19 PM
Formatted: Font:Not Italic

Table 6 summarizes the submicron absorption results averaged over all ARCTAS phases for the different BC mixing rules that can be used in ASP v2.1. The relatively poor correlation and wide spread of errors is consistent across mixing rules. As expected, the assumption of an external mixture (EXT) results in the lowest modeled absorption, significantly underestimating absorption at 470 nm and 532 nm, but giving very little bias at 660 nm. In contrast, the internal mixtures (CS, MG, and VA) all overestimate absorption, but show much less dependence of this bias on wavelength. CS and VA both give regression slopes near 1, but the VA mixing rule shows a larger overestimate of absorption than the CS mixing rule, while the MG mixing rule has a lower positive bias than CS.

Matthew Alvarado 5/27/2016 7:19 PM
Deleted:

Matthew Alvarado 11/17/2015 3:28 PM
Deleted: Table 6

Matthew Alvarado 5/24/2016 3:05 PM
Deleted: states

Matthew Alvarado 5/24/2016 3:05 PM
Deleted: states

Matthew Alvarado 5/24/2016 3:05 PM
Deleted: state

Matthew Alvarado 5/24/2016 3:05 PM
Deleted: state

Matthew Alvarado 5/24/2016 3:05 PM
Deleted: state

However, the results vary significantly between the different phases of ARCTAS. For example, Figure 9 shows the histograms of the ASP errors when the CS mixing rule is used

Matthew Alvarado 11/17/2015 3:28 PM
Deleted: Figure 9

Matthew Alvarado 5/24/2016 3:05 PM
Deleted: state

separated for the three campaigns. We can see that both the mean bias and the spread of the errors vary significantly between the campaigns. For example, ASP with CS appears relatively unbiased for ARCTAS-CARB (μ = -0.02) but the spread of the errors is large (σ = 0.36). The results for ARCTAS-A show a small positive bias (μ = 0.07) similar to the overall GMI results (μ = 0.06, see Table 3), but with a small spread in the errors (σ = 0.18). In contrast, ASP with CS substantially overestimates absorption during ARCTAS-B by an average factor of 2 (μ = 0.32), but again shows a relatively small spread of errors (σ = 0.23).

These differences between the campaigns make sense when we consider the types of pollution sampled during each campaign. ARCTAS-A sampled primarily aged Arctic haze particles, and so the BC in these particles would be expected to be internally mixed. In contrast, ARCTAS-B sampled substantial amounts of fresh biomass burning smoke, where about half of the BC would be expected to be externally mixed (e.g., Akagi et al., 2012) and thus have lower absorption per mass of BC than would be calculated by the core-shell assumption. Finally, ARCTAS-CARB sampled a mixture of anthropogenic pollution and biomass burning smoke from a variety of sources. These aerosols are likely in a variety of mixing states and have a variety of size distributions of BC particles, and thus ASP CS would be expected to show the large spread of errors seen. These results do not definitively prove that the difference in the performance of ASP v2.1 for the three ARCTAS campaigns is due to errors in mixing state, but they do suggest the need for further development of the ASP model to allow for time-varying mixing states and to allow the BC size distribution to vary independently of the overall size distribution.

In order to examine the benefit that including a time-varying mixing state for BC in ASP could bring, we examined a third “variable” mixing rule case where CS was used for ARCTAS-A and ARCTAS-CARB while EXT was used for ARCTAS-B. The results are shown in Figure 10 and Table 6. This variable mixing rule generally shows lower mean positive biases than any of the internally-mixed rules (CS, VA, MG) while showing a slightly smaller spread in the errors than any of the constant mixing rule cases (σ of 0.28-0.29 versus 0.30-0.32), more consistent with the GMI results seen in Table 3. However, the correlation coefficient is still very poor (r^2 = 0.44-0.45), suggesting that the assumption in ASP v2.1 of a constant mixing ratio of BC throughout the overall size distribution can lead to errors in submicron aerosol absorption as large as those seen in the externally-mixed, fixed-size distribution global models.

Matthew Alvarado 11/17/2015 3:28 PM
Deleted: Table 3

Matthew Alvarado 5/27/2016 8:40 PM
Deleted: point to

Matthew Alvarado 5/24/2016 3:06 PM
Deleted: state

Matthew Alvarado 11/17/2015 3:28 PM
Deleted: Figure 10

Matthew Alvarado 11/17/2015 3:28 PM
Deleted: Table 6

Matthew Alvarado 5/24/2016 3:06 PM
Deleted: state

Matthew Alvarado 5/24/2016 3:06 PM
Deleted: states

Matthew Alvarado 5/24/2016 3:06 PM
Deleted: state

Matthew Alvarado 11/17/2015 3:28 PM
Deleted: Table 3

Table 7 summarizes the results for SSA for ASP v2.1 using different mixing rules. When assuming internal mixtures, ASP tends to underestimate the SSA by an average of 0.01 to 0.04, while assuming external mixtures gives fairly unbiased results (-0.01 to 0.01). We see that the “variable” mixing rule gives small negative biases similar to the results from the MG mixing rule, but has a higher correlation coefficient (r^2 of 0.30 at 532 nm, compared to 0.20 for MG). The SSA correlation coefficients for ASP v2.1 for all mixing rules are generally higher than those for GMI or GEOS-Chem v9-02.

Matthew Alvarado 11/17/2015 3:28 PM
Deleted: Table 7

Matthew Alvarado 5/24/2016 3:06 PM
Deleted: states

Matthew Alvarado 5/24/2016 3:06 PM
Deleted: state

Matthew Alvarado 5/24/2016 3:06 PM
Deleted: state

Matthew Alvarado 5/24/2016 3:06 PM
Deleted: states

7 Conclusions

We performed a closure study using in situ observations of submicron aerosol concentration, composition, size distribution, scattering, and absorption from the NASA ARCTAS campaign to evaluate the modeling of submicron aerosol scattering and absorption in four global parameterizations (those used in the GMI Combo model, OPAC v3.1, GEOS-Chem v9-02, and the baseline configuration of GC-RT) as well as the smoke plume chemistry model ASP v2.1. Our closure study allowed for the evaluation of the predictions of aerosol scattering and absorption by these models without the complications associated with different treatments of aerosol emissions, transport, chemistry, and deposition. We find that the GMI model has smaller mean biases in predicting submicron aerosol scattering and absorption than OPAC v3.1, GEOS-Chem v9-02, or the baseline GC-RT. The better performance of GMI for absorption seems to be primarily due to the assumption of a larger density for BC (1.5 g cm^{-3}) than in OPAC v3.1, as the size distribution and refractive index for BC are the same for these models. On average, GMI overestimates submicron aerosol scattering during ARCTAS by 15% (1σ range -34% to 100%) at 450 nm and 23% (-29% to 114%) at 550 nm, while it underestimates scattering at 700 nm by -11% (-53% to 66%). When the Lack et al. (2008) correction is applied to the ARCTAS PSAP observations, GMI overestimates submicron aerosol absorption by 10% (1σ range -41% to 104%) at 470 nm, by 15% (-38% to 114%) at 532 nm, and by 0% (-42% to 74%) at 660 nm. On average GMI slightly overestimates mean submicron SSA during ARCTAS (0.01 ± 0.05 at 470 and 532 nm, 0.02 ± 0.07 at 660 nm) while GEOS-Chem v9-02 slightly underestimates it (-0.01 ± 0.05 at 470 and 532 nm, -0.02 ± 0.06 at 660 nm), but the correlation is very poor for all models, suggesting that while the mean is reasonable the models tend to have little skill predicting individual data points. We also find that the changes to the treatment of BC in the baseline configuration of GC-RT reduce the positive bias in modeled absorption relative to that in GEOS-Chem v9-02 (e.g.,

Matthew Alvarado 5/25/2016 9:52 AM
Formatted: Superscript

from a mean overestimate of 86% in GEOS-Chem v9-02 to a mean overestimate of 66% at 532 nm). This is likely due to a net reduction in BC absorption due to the increase in the assumed density of BC (1.0 g cm^{-3} in GEOS-Chem v9-02, 1.8 g cm^{-3} in GC-RT) that is partially offset by the increased imaginary refractive index for BC in GC-RT.

The use of in situ size distribution information allows ASP v2.1 to accurately simulate submicron aerosol scattering with a high correlation (r^2 = 0.88-0.89) and very little spread in the error distribution compared to the GMI model. When a core-shell (CS) BC mixing rule is used, ASP v2.1 underestimates aerosol scattering during ARCTAS by 7% (1σ range -37% to 38%) at 450 and 550 nm and 2% (-34% to 45%) at 700 nm on average. However, the ASP v2.1 results for submicron aerosol absorption show a substantially lower correlation (r^2 = 0.44-0.50) likely due to the assumption in ASP v2.1 of a constant mass fraction of BC throughout the size distribution. When a CS mixing rule is used, ASP v2.1 overestimates submicron aerosol absorption by 29 to 35% with a weak dependence on wavelength, while ASP v2.1 with an external (EXT) mixture in ASP tends to underestimate aerosol absorption, with the average errors showing a strong dependence on wavelength (-21% at 470 nm, -11% at 532 nm, and 0% at 660 nm). Examination of the distribution of errors for each phase of the ARCTAS campaign suggests that an external mixture is best for the fresh smoke observations in ARCTAS-B, while an internally mixed core-shell approach is better for the aged Arctic haze in ARCTAS-A and the anthropogenic pollution in ARCTAS-CARB. Using this “variable” mixing rule in ASP v2.1 leads to an average overestimate of aerosol absorption of 10% (1σ range -42% to 109%) at 470 nm, 17% (-38% to 124%) at 532 nm, and 23% (-37% to 140%) at 660 nm.

These results suggest that the GMI model performs the best of the four fixed size distribution schemes evaluated here in simulating submicron aerosol scattering and absorption, and that future refinements to the GMI approach should focus on improvements that, on average, reduce scattering and absorption in the 550/532 nm and 450/470 nm bands. Increasing the density of OC in GMI to 1.8 g cm^{-3} to match the other fixed-sixe distribution models would likely reduce all three wavelengths equally, and the changes to the fixed size distribution parameters examined here generally resulted in stronger absorption and scattering in all wavelengths, so refining the wavelength dependence of the complex refractive indices used in GMI might be the most promising pathway for significant improvements. For GEOS-Chem, adopting the baseline GC-RT BC parameters from Wang et al. (2014) for the standard GEOS-

Matthew Alvarado 5/25/2016 9:50 AM
Formatted: Superscript

Matthew Alvarado 5/25/2016 9:49 AM
Formatted: Font:

Matthew Alvarado 5/24/2016 3:07 PM
Deleted: state

Matthew Alvarado 5/24/2016 3:07 PM
Deleted: state

Matthew Alvarado 5/24/2016 3:07 PM
Deleted: state

Matthew Alvarado 5/24/2016 4:35 PM
Deleted: does a reasonable job modeling

Matthew Alvarado 5/25/2016 11:18 AM
Formatted: Superscript

Chem model would substantially improve the ability of the model to simulate aerosol absorption. However, further refinements to the treatment of BC and OA absorption are needed to reduce the positive bias that remains in GC-RT, such as the potential of BrC absorption to decrease with atmospheric age (e.g., Forrester et al., 2015). For ASP v2.1, the results show that future model development should focus on improvements to the simulation of submicron aerosol absorption by adding routines that allow for a more complete description of aerosol mixing state (such as in the PartMC-MOSAIC model, Tian et al., 2014) and adding the ability for the BC mass fraction to vary with aerosol size. In addition, similar closure studies should be performed with data from other recent field campaigns, such as NASA Studies of Emissions and Atmospheric Composition, Clouds and Climate Coupling by Regional Surveys (SEAC^{4}RS; Toon, 2013) and the US Department of Energy Biomass Burning Observation Project (BBOP; Kleinman et al., 2014) campaign, to investigate how the biases in the aerosol optical property models vary with location and pollution source.

Acknowledgements

The authors thank the other members of the ARCTAS Science Team. We also thank Prof. Rodney Weber of the Georgia Institute of Technology for the use of his PILS data, as well as Prof. Christopher Cappa of the University of California - Davis and Dr. Manvendra Dubey of Los Alamos National Laboratory for their helpful comments. This analysis and associated updates to the ASP model were funded under NASA Grant NNX11AN72G to MJA, CRL, HLM, HB, MC, and CW, as well as NSF Grant AGS-1144165 to MJA and CRL. DAR and CLH were partially supported by NASA grant NN14AP38G. JLJ was partially supported by NASA NNX15AT96G and NNX15AH33A. The contribution of JED to ARCTAS was supported by NASA grant NNX08AH69G.

References

Alvarado, M. J.: Formation of Ozone and Growth of Aerosols in Young Smoke Plumes from Biomass Burning, Ph.D. Thesis, Massachusetts Institute of Technology, Cambridge, MA, USA, 324 pp., available at http://globalchange.mit.edu/files/document/Alvarado_PhD_08.pdf, 2008.

Alvarado, M. J. and Prinn, R. G.: Formation of ozone and growth of aerosols in young smoke plumes from biomass burning: 1. Lagrangian parcel studies, J. Geophys. Res., 114, D09306, doi:10.1029/2008JD011144, 2009.

Alvarado, M. J., Wang, C., and Prinn, R. G.: Formation of ozone and growth of aerosols in young smoke plumes from biomass burning: 2. Three-dimensional Eulerian studies, J. Geophys. Res., 114, D09307, doi:10.1029/2008JD011186, 2009.

Alvarado, M. J., Lonsdale, C. R., Yokelson, R. J., Akagi, S. K., Coe, H., Craven, J. S., Fischer, E. V., McMeeking, G. R., Seinfeld, J. H., Soni, T., Taylor, J. W., Weise, D. R., and Wold, C. E.: Investigating the Links Between Ozone and Organic Aerosol Chemistry in a Biomass Burning Plume from a Prescribed Fire in California Chaparral, Atmos. Chem. Phys., 15, 6667–6688, doi:10.5194/acp-15-6667-2015, 2015.

Anderson, B. E., Cofer, W. R., Bagwell, D. R., Barrick, J. W., Hudgins, C. H., Brunke, K. E.: Airborne observations of aircraft aerosol emissions 1: total nonvolatile particle emission indices, Geophys. Res. Lett., 25, 1689–1692, 1998.

Anderson, T. L. and Ogren, J. A.: Determining Aerosol Radiative Properties Using the TSI 3563 Integrating Nephelometer, Aerosol Science and Technology, 29, 57–69, doi:10.1080/02786829808965551, 1998.

Andreae, M. O. and Gelencsér, A.: Black carbon or brown carbon? The nature of light-absorbing carbonaceous aerosols, Atmos. Chem. Phys., 6, 3131–3148, doi:10.5194/acp-6-3131–2006, 2006.

Bahreini, R. Ervens, B., Middlebrook, A. M., Warneke, C., de Gouw, J. A., DeCarlo, P. F., Jimenez, J. L., Atlas, E., Brioude, J., Brock, C. A., Fried, A., Holloway, J. S., Peischl, J., Richter, D., Ryerson, T. B., Stark, H., Walega, J., Weibring, P., Wollny, A. G., and Fehsenfeld, F. C.: Organic Aerosol Formation in Urban and Industrial plumes near Houston and Dallas, TX, J. Geophys. Res., 114, D00F16, doi:10.1029/2008JD011493, 2009.

Bey, I., Jacob, D. J., Yantosca, R. M., Logan, J. A., Field, B. D., Fiore, A. M., Li, Q., Liu, H. Y., Mickley, L. J., and Schultz, M. G.: Global modeling of tropospheric chemistry with assimilated meteorology: Model description and evaluation, J. Geophys. Res., 106, 23073–23078, 2001.

Bian, H., Prather, M. J., and Takemura, T.: Tropospheric aerosol impacts on trace gas budgets through photolysis, J. Geophys. Res., 108, 4242, doi:10.1029/2002JD002743, 2003.

Bond, T. C. and Bergstrom, R. W.: Light absorption by carbonaceous particles: an investigative review, Aerosol Sci. Tech., 40, 27–67, doi:10.1080/02786820500421521, 2006.

Bond, T. C., Doherty, S. J., Fahey, D. W., Forster, P. M., Berntsen, T., DeAngelo, B. J., Flanner, M. G., Ghan, S., Kärcher, B., Koch, D., Kinne, S., Kondo, Y., Quinn, P. K., Sarofim, M. C., Schultz, M. G., Schulz, M., Venkataraman, C., Zhang, H., Zhang, S., Bellouin, N., Guttikunda, S. K., Hopke, P. K., Jacobson, M. Z., Kaiser, J. W., Klimont, Z., Lohmann, U., Schwarz, J. P., Shindell, D., Storelvmo, T., Warren, S. G., and Zender, C. S.: Bounding the role of black carbon in the climate system: A scientific assessment, J. Geophys. Res., 118, 5380–5552, doi:10.1002/jgrd.50171, 2013.

Canagaratna, M.R., Jayne, J.T., Jimenez, J.L., Allan, J.D., Alfarra, M.R, Zhang, Q., Onasch, T.B., Drewnick, F., Coe, H., Middlebrook, A., Delia, A., Williams, L.R., Trimborn, A.M., Northway, M.J., DeCarlo, P.F., Kolb, C.E., Davidovits, P., Worsnop, D.R. Chemical and Microphysical Characterization of Ambient Aerosols with the Aerodyne Aerosol Mass Spectrometer. Mass Spectrometry Reviews, 26, 185– 222, 2007.

Cai, Y., Montague, D. C., and Deshler, T.: Comparison of measured and calculated scattering from surface aerosols with an average, a size-dependent, and a time-dependent refractive index, J. Geophys. Res., 116, D02202, doi:10.1029/2010JD014607, 2011.

Cappa, C. D., Onasch, T. B., Massoli, P., Worsnop, D. R., Bates, T. S., Cross, E. S., Davidovits, P., Hakala, J., Hayden, K. L., Jobson, B. T., Kolesar, K. R., Lack, D. A., Lerner, B. M., Li, S.-M., Mellon, D., Nuaaman, I., Olfert, J. S., Petäjä, T., Quinn, P. K., Song, C., Subramanian, R., Williams, E. J., and Zaveri, R. A.: Radiative Absorption Enhancements Due to the Mixing State of Atmospheric Black Carbon, Science, 337, 1078–1081, doi:10.1126/science.1223447, 2012.

Chin, M., Ginoux, P., Kinne, S., Holben, B. N., Duncan, B. N., Martin, R. V., Logan, J. A., Higurashi, A., and Nakajima, T.: Tropospheric aerosol optical thickness from the GOCART

Matthew Alvarado 5/25/2016 3:00 PM
Formatted: Font:Not Italic

Matthew Alvarado 5/25/2016 3:00 PM
Formatted: Font:Not Italic

Matthew Alvarado 5/25/2016 3:00 PM
Formatted: Font:Not Italic

Matthew Alvarado 5/25/2016 3:00 PM
Formatted: Font:Not Italic

Unknown
Field Code Changed

Matthew Alvarado 5/25/2016 3:00 PM
Formatted: Font:Not Italic

Matthew Alvarado 5/25/2016 3:00 PM
Formatted: Font:Not Italic

model and comparisons with satellite and sun photometer measurements, J. Atmos. Sci., 59, 461–483, 2002.

Chin, M., Diehl, T., Dubovik, O., Eck, T. F., Holben, B. N., Sinyuk, A., and Streets, D. G., Light absorption by pollution, dust, and biomass burning aerosols: a global model study and evaluation with AERONET measurements, Ann. Geophys., 27, 3439–3464, doi:10.5194/angeo-27-3439-2009, 2009.

Chung, C. E., Ramanathan, V., and Decremer, D.: Observationally constrained estimates of carbonaceous aerosol radiative forcing, PNAS, 109, 11624–11629, doi:10.1073/pnas.1203707109, 2012.

Cubison, M. J., Ortega, A. M., Hayes, P. L., Farmer, D. K., Day, D., Lechner, M. J., Brune, W. H., Apel, E., Diskin, G. S., Fisher, J. A., Fuelberg, H. E., Hecobian, A., Knapp, D. J., Mikoviny, T., Riemer, D., Sachse, G. W., Sessions, W., Weber, R. J., Weinheimer, A. J., Wisthaler, A., and Jimenez, J. L.: Effects of aging on organic aerosol from open biomass burning smoke in aircraft and laboratory studies, Atmos. Chem. Phys., 11, 12049-12064, doi:10.5194/acp-11-12049-2011, 2011.

DeCarlo, P., Slowik, J.G., Worsnop, D.R., Davidovits, P., and Jimenez, J.L. Particle Morphology and Density Characterization by Combined Mobility and Aerodynamic Diameter Measurements. Part 1: Theory. Aerosol Science and Technology, 38: 1185–1205, 2004. DOI: 10.1080/027868290903907.

DeCarlo, P. F., Dunlea, E. J., Kimmel, J. R., Aiken, A. C., Sueper, D., Crounse, J., Wennberg, P. O., Emmons, L., Shinozuka, Y., Clarke, A., Zhou, J., Tomlinson, J., Collins, D. R., Knapp, D., Weinheimer, A. J., Montzka, D. D., Campos, T., and Jimenez, J. L.: Fast airborne aerosol size and chemistry measurements above Mexico City and Central Mexico during the MILAGRO campaign, Atmos. Chem. Phys., 8, 4027–4048, doi:10.5194/acp-8-4027–2008, 2008.

Dibb, J. E., Talbot, R. W., Scheuer, E., Seid, G., Avery, M. A., and Singh, H. B.: Aerosol chemical composition in Asian continental outflow during TRACE-P: Comparison to PEM-West B, J. Geophys. Res., 108 (D21), 8815, doi:10.1029/2002JD003111, 2003.

Drury, E. E., Jacob, D. J., Spurr, R. J. D., Wang, J., Shinozuka, Y., Anderson, B. E., Clarke, A. D., Dibb, J., McNaughton, C., and Weber, R. J.: Synthesis of satellite (MODIS), aircraft (ICARTT), and surface (IMPROVE, EPA-AQS, AERONET) aerosol observations over eastern North America to improve MODIS aerosol retrievals and constrain aerosol concentrations and sources, J. Geophys. Res., 115, D14204, doi:10.1029/2009JD012629, 2010.

Dubovik, O. and King, M. D.: A flexible inversion algorithm for retrieval of aerosol optical properties from Sun and sky radiance measurements, J. Geophys. Res., 105, 20673–20696, 2000.

Duncan, B. N., Strahan, S. E., Yoshida, Y., Steenrod, S. D., and Livesey, N.: Model study of the cross-tropopause transport of biomass burning pollution, Atmos. Chem. Phys., 7, 3713–3736, doi:10.5194/acp-7-3713-2007, 2007.

Esteve, A. R., Highwood, E. J., Morgan, W. T., Allen, G., Coe, H., Grainger, R. G., Brown, P., and Szpek, K.: A study on the sensitivities of simulated aerosol optical properties to composition and size distribution using airborne measurements, Atmos. Environ., 89, 517-524, doi:10.1016/j.atmosenv.2014.02.063, 2014.

Fredenslund, A., J. Gmehling, and P. Rasmussen, Vapor-Liquid Equilibria Using UNIFAC, A Group Contribution Method, Elsevier, Amsterdam, 1977.

Forrister, H., Liu, J., Scheuer, E., Dibb, J., Ziemba, L., Thornhill, K. L., Anderson, B., Diskin, G., Perring, A. E., Schwarz, J. P., Campuzano-Jost, P., Day, D. A., Palm, B. B., Jimenez, J. L., Nenes, A., and Weber, R. J.: Evolution of brown carbon in wildfire plumes. Geophys. Res. Lett., 42, 4623–4630. doi: 10.1002/2015GL063897, 2015.

Fountoukis, C. and Nenes, A.: ISORROPIA II: A computationally efficient thermodynamic equilibrium model for K^+–Ca^{2+}–Mg^{2+}–NH_4^+–Na^+–SO_4^{2-}–NO_3^-–Cl^-–H_2O aerosols, Atmospheric Chemistry and Physics, 7, 4639–4659, 2007.

Ginoux, P., Chin, M., Tegen, I., Prospero, J., Holben, B., Dubovik, O., and Lin, S.-J.: Sources and global distributions of dust aerosols simulated with the GOCART model, J. Geophys. Res., 106, 20,255–20,273, 2001.

Ginoux, P., Prospero, J., Torres, O., and Chin, M.: Long-term simulation of dust distribution with the GOCART model: Correlation with the North Atlantic Oscillation, Environ. Modeling and Software, 19, 113–128, 2004.

He, S., and Carmichael, G.: Sensitivity of photolysis rates and O_3 production in the troposphere to aerosol properties, J. Geophys. Res., 104, 26307–26324, 1991.

Heald, C. L., Ridley, D. A., Kroll, J. H., Barrett, S. R. H., Cady-Pereira, K. E., Alvarado, M. J., and Holmes, C. D.: Contrasting the direct radiative effect and direct radiative forcing of aerosols, Atmos. Chem. Phys., 14, 5513–5527, doi:10.5194/acp-14-5513-2014, 2014.

Hess, M., Koepke, P., and Schult, I.: Optical Properties of Aerosols and clouds: The software package OPAC, Bull. Am. Met. Soc., 79, 831–844, 1998.

Highwood, E. J., Northway, M. J., McMeeking, G. R., Morgan, W. T., Liu, D., Osborne, S., Bower, K., Coe, H., Ryder, C., and Williams, P.: Aerosol scattering and absorption during the EUCAARI-LONGREX flights of the Facility for Airborne Atmospheric Measurements (FAAM) BAe-146: can measurements and models agree?, Atmos. Chem. Phys., 12, 7251-7267, doi:10.5194/acp-12-7251-2012, 2012.

Huffman, J. A., Jayne, J. T., Drewnick, F., Aiken, A. C., Onasch, T., Worsnop, D. R., and Jimenez, J. L.: Design, Modeling, Optimization, and Experimental Tests of a Particle Beam Width Probe for the Aerodyne Aerosol Mass Spectrometer, Aerosol Sci. and Technol., 39, 1143-1163, doi:10.1080/02786820500423782, 2005.

Iacono, M. J., Delamere, J. S., Mlawer, E. J., Shephard, M. W., Clough, S. A., and Collins, W. D.: Radiative forcing by long-lived greenhouse gases: calculations with the AER radiative transfer models, J. Geophys. Res.-Atmos., 113, D13103, doi:10.1029/2008jd009944, 2008.

Jacob, D. J., Crawford, J. H., Maring, H., Clarke, A. D., Dibb, J. E., Emmons, L. K., Ferrare, R. A., Hostetler, C. A., Russell, P. B., Singh, H. B., Thompson, A. M., Shaw, G. E., McCauley, E., Pederson, J. R., and Fisher, J. A.: The Arctic Research of the Composition of the Troposphere from Aircraft and Satellites (ARCTAS) mission: design, execution, and first results, Atmos. Chem. Phys., 10, 5191–5212, doi:10.5194/acp-10-5191-2010, 2010.

Jacobson, M. Z.: Development and application of a new air pollution modeling system - II. Aerosol module structure and design, Atmos. Environ., 31, 131–144, 1997.

Jacobson, M. Z.: Studying the effects of aerosols on vertical photolysis rate coefficient and temperature profiles over an urban airshed, J. Geophys. Res., 103, 10593–10604, 1998.

Jacobson, M. Z.: Strong radiative heating due to the mixing state of black carbon in atmospheric aerosols, Nature, 409, 695–697, 2001.

Matthew Alvarado 5/24/2016 5:13 PM
Formatted: Default Paragraph Font, Font color: Auto, German

Matthew Alvarado 5/24/2016 5:13 PM
Formatted: Default Paragraph Font, Font color: Auto, German

Jacobson, M. Z.: Analysis of aerosol interactions with numerical techniques for solving coagulation, nucleation, condensation, dissolution, and reversible chemistry among multiple size distributions, J. Geophys. Res., 107, 4366, doi:10.1029/2001JD002,044, 2002.

Jacobson, M. Z.: Fundamentals of Atmospheric Modeling, 2nd ed., Cambridge University Press, 2005.

Jaeglé, L., Quinn, P. K., Bates, T. S., Alexander, B., and Lin, J.-T.: Global distribution of sea salt aerosols: new constraints from in situ and remote sensing observations, Atmos. Chem. Phys., 11, 3137–3157, doi:10.5194/acp-11-3137-2011, 2011.

Jimenez, J. L., Canagaratna, M. R., Donahue, N. M., Prevot, A. S. H., Zhang, Q., Kroll, J. H., DeCarlo, P. F., Allan, J. D., Coe, H., Ng, N. L., Aiken, A. C., Docherty, K. S., Ulbrich, I. M., Grieshop, A. P., Robinson, A. L., Duplissy, J., Smith, J. D., Wilson, K. R., Lanz, V. A., Hueglin, C., Sun, Y. L., Tian, J., Laaksonen, A., Raatikainen, T., Rautiainen, J, Vaattovaara, P., Ehn, M., Kulmala, M., Tomlinson, J. M., Collins, D. R., Cubison, M. J., Dunlea, E. J., Huffman, J. A., Onasch, T. B., Alfarra, M. R., Williams, P. I., Bower, K., Kondo, Y., Schneider, J., Drewnick, F., Borrmann, S., Weimer, S., Demerjian, K., Salcedo, D., Cottrell, L., Griffin, R., Takami, A., Miyoshi, T, Hatakeyama, S., Shimono, A., Sun, J. Y., Zhang, Y. M., Dzepina, K., Kimmel, J. R., Sueper, D., Jayne, J. T., Herndon, S. C., Trimborn, A. M., Williams, L. R., Wood, E. C., Middlebrook, A. M., Kolb, C. E., Baltensperger, U., and Worsnop, D. R.: Evolution of Organic Aerosols in the Atmosphere, Science, 326,1525–1529, 2009.

Kassianov, E., Berg, L. K., Pekour, M., Barnard, J., Chand, D., Flynn, C., Ovchinnikov, M., Sedlacek, A., Schmid, B., Shilling, J., Tomlinson, J., and Fast, J.: Airborne aerosol in situ measurements during TCAP: A closure study of total scattering. Atmosphere, 6, 1069-1101, doi:10.3390/atmos6081069, 2015.

Matthew Alvarado 6/16/2016 3:24 PM
Formatted: Font:Not Italic

Matthew Alvarado 6/16/2016 3:24 PM
Formatted: Font:Not Italic

Kim, D., Wang, C., kman, A. M. L., Barth, M. C., and Rasch, P. J.: Distribution and direct radiative forcing of carbonaceous and sulfate aerosols in an interactive size-resolving aerosol–climate model, J. Geophys. Res., 113, D16309, doi:10.1029/2007JD009756, 2008.

Kim, Y. P., Seinfeld, J. H., and Saxena, P.: Atmospheric gas-aerosol equilibrium I. thermodynamic model, Aerosol Science and Technology, 19, 157–181, 1993.

Kleinman, L. I., Sedlacek, A. J., III, Yokelson, R. J., Onasch, T. B., Adachi, K., Buseck, P. R., Chand, D., Collier, S., Dubey, M. K., Mei, F., Shilling, J. E., Springston, S. R., Wang, J., Wigder, N. L., and Zhang, Q.: Time Dependence of Aerosols in Biomass Burn Plumes from BBOP, American Geophysical Union, Fall Meeting 2014, Abstract #A52A-01, 2014.

Kondo, Y., Oshima, N., Kajino, M., Mikami, R., Moteki, N., Takegawa, N., Verma, R. L., Kajii, Y., Kato, S., and Takami, A.: Emissions of black carbon in East Asia estimated from observations at a remote site in the East China Sea, J. Geophys. Res., 116, D16201, doi:10.1029/2011JD015637, 2011.

Kusik, C., and Meissner, H.: Electrolyte activity coefficients in inorganic processing, in Fundamental Aspects of Hydrometallurgical Processes, AIChE Symposium Series, edited by T. Chapman, L. Taularides, G. Hubred, and R. Wellek, pp. 14–20, AIChE, New York, 1978.

Lack, D. A., Cappa, C. D., Covert, D. S., Baynard, T., Massoli, P., Sierau, B., Bates, T. S., Quinn, P. K., Lovejoy, E. R., and Ravishankara, A. R.: Bias in Filter-Based Aerosol Light Absorption Measurements Due to Organic Aerosol Loading: Evidence from Ambient Measurements, Aerosol Science and Technology, 42, 1033–1041, doi:10.1080/02786820802389277, 2008.

Lack, D. A. and Cappa, C. D.: Impact of brown and clear carbon on light absorption enhancement, single scatter albedo and absorption wavelength dependence of black carbon, Atmos. Chem. Phys., 10, 4207–4220, doi:10.5194/acp-10-4207-2010, 2010.

Lack, D. A., J. M. Langridge, R. Bahreini, C. D. Cappa, A. M. Middlebrook, and J. P. Schwarz. Brown carbon and internal mixing in biomass burning particles, PNAS, 109, 14802-14807, doi:10.1073/pnas.1206575109, 2012.

Lefer, B. L., Shetter, R. E., Hall, S. R., Crawford, J. H., and J. R.: Impact of clouds and aerosols on photolysis frequencies and photochemistry during TRACE-P: 1. Analysis using radiative transfer and photochemical box models, J. Geophys. Res., 108, 8821, doi:10.1029/2002JD003171, 2003.

Li, G., Zhang, R., Fan, J., and Tie, X.: Impacts of black carbon aerosol on photolysis and ozone, J. Geophys. Res., 110, D23206, doi:10.1029/2005JD005898, 2005.

Liao, H., Yung, Y., and Seinfeld, J.: Effects of aerosols on tropospheric photolysis rates in clear and cloudy atmospheres, J. Geophys. Res., 104(D19), 23697–23707, 1999.

Liao, H., Adams, P. J., Seinfeld, J. H., Mickley, L. J. and Jacob D. J.: Interactions between tropospheric chemistry and aerosols in a unified GCM simulation, J. Geophys. Res., 108(D1), 4001, doi:10.1029/2001JD001260, 2003.

Liu, X., Penner, J. E., Das, B., Bergmann, D., Rodriguez, J. M., Strahan, S., Wang, M., and Feng, Y.: Uncertainties in global aerosol simulations: Assessment using three meteorological data sets, J. Geophys. Res., 112, D11212, doi:10.1029/2006JD008216, 2007.

Loeb, N. G. and Su, W.: Direct aerosol radiative forcing uncertainty based on a radiative perturbation analysis, J. Climate 23, 5288-5293, doi:10.1175/2010JCLI3543.1, 2010.

Martin, R. V., Jacob, D. J., Yantosca, R. M., Chin, M., and Ginoux, P.: Global and regional decreases in tropospheric oxidants from photochemical effects of aerosols, J. Geophys. Res., 108, 4097, doi:10.1029/2002JD002622, 2003.

Maxwell Garnet, J. C.: Colours in metal glasses and in metallic films, Philos. Trans. Roy. Soc. A203, 385–420, 1904.

Michelangeli, D., Allen, M., Yung, Y., Shia, R.-L., Crisp, D., and Eluszkiewicz, J.: Enhancement of Atmospheric Radiation by an Aerosol Layer, J. Geophys. Res., 97(D1), 865–874, 1992.

Moteki, N. and Kondo, Y.: Effects of mixing state on black carbon measurements by Laser-Induced Incandescence, Aerosol Sci. Technol., 41, 398–417, 2007.

Moteki, N. and Kondo, Y.: Method to measure time-dependent scattering cross sections of particles evaporating in a laser beam, J. Aerosol Sci., 39, 348–364, 2008.

Myrdal, P. B. and Yalkowsky, S. H.: Estimating pure component vapor pressures of complex organic molecules, Industrial and Engineering Chemistry Research, 36, 2494–2499, 1997.

Nenes, A., Pandis, S. N., and Pilinis, C.: ISORROPIA: A new thermodynamic equilibrium model for multiphase multicomponent inorganic aerosols, Aquatic Geochemistry, 4, 123–152, 1998.

Park, R. J., Jacob, D. J., Chin, M., and Martin, R. V.: Sources of carbonaceous aerosols over the United States and implications for natural visibility, J. Geophys. Res., 108, 4355, doi:10.1029/2002JD003190, 2003.

Matthew Alvarado 5/27/2016 9:22 PM
Formatted: Default Paragraph Font

Petters, M. D., and Kreidenweis, S. M.: A single parameter representation of hygroscopic growth and cloud condensation nucleus activity, Atmos. Chem. Phys., 7, 1961–1971, doi:10.5194/acp-7-1961-2007, 2007.

Pun, B. K., Griffin, R. J., Seigneur, C., and Seinfeld, J. H.: Secondary organic aerosol, 2, thermodynamic model for gas/particle partitioning of molecular constituents, J. Geophys. Res., 107, 4333, doi:10.1029/2001JD000,542, 2002.

Quinn, P. K., and Coffman, D. J.: Local closure during the First Aerosol Characterization Experiment (ACE 1): Aerosol mass concentration and scattering and backscattering coefficients, J. Geophys. Res., 103, 16575–16596, doi:10.1029/97JD03757, 1998.

Reid, J. S., Brooks, B., Crahan, K. K., Hegg, D. A., Eck, T. F., O'Neill, N., de Leeuw, G., Reid, E. A., and Anderson, K. D.: Reconciliation of coarse mode sea-salt aerosol particle size measurements and parameterizations at a subtropical ocean receptor site, J. Geophys. Res., 111, D02202, doi:10.1029/2005JD006200, 2006.

Schwarz, J. P., Spackman, J. R., Fahey, D. W., Gao, R. S., Lohmann, U., Stier, P., Watts, L. A., Thomson, D. S., Lack, D. A., Pfister, L., Mahoney, M. J., Baumgardner, D., Wilson, J. C., and Reeves, J. M.: Coatings and their enhancement of black carbon light absorption in the tropical atmosphere, J. Geophys. Res., 113, D03203, doi:10.1029/2007JD009042, 2008.

Sciare, J., Oikonomou, K., Cachier, H., Mihalopoulos, N., Andreae, M. O., Maenhaut, W., and Sarda-Estève, R.: Aerosol mass closure and reconstruction of the light scattering coefficient over the Eastern Mediterranean Sea during the MINOS campaign, Atmos. Chem. Phys., 5, 2253-2265, doi:10.5194/acp-5-2253-2005, 2005.

Shiraiwa, M., Kondo, Y., Iwamoto, T., and Kita, K.: Amplification of Light Absorption of Black Carbon by Organic Coating, Aerosol Sci. Tech., 44, 46–54, 2010.

Steele, H. D., Investigations of cloud altering effects of atmospheric aerosols using a new mixed eulerian-lagrangian aerosol model, Ph.D. thesis, Massachusetts Institute of Technology, 2004.

Stier, P., Seinfeld, J. H., Kinne, S., Feichter, J., and Boucher, O.: Impact of nonabsorbing anthropogenic aerosols on clearsky atmospheric absorption, J. Geophys. Res., 111, D18201, doi:10.1029/2006JD007147, 2006.

Matthew Alvarado 5/25/2016 2:43 PM
Formatted: Font:Not Italic

Matthew Alvarado 5/25/2016 2:43 PM
Formatted: Font:Not Italic

Matthew Alvarado 5/25/2016 2:43 PM
Formatted: Font:Not Italic

Unknown
Field Code Changed

Matthew Alvarado 5/25/2016 2:43 PM
Formatted: Font:Not Italic

Matthew Alvarado 5/25/2016 2:43 PM
Formatted: Font:Not Italic

Matthew Alvarado 5/25/2016 2:58 PM
Formatted: English (US)

Strahan, S. E., Duncan, B. N., and Hoor, P.: Observationally derived transport diagnostics for the lowermost stratosphere and their application to the GMI chemistry and transport model, Atmos. Chem. Phys., 7, 2435–2445, doi:10.5194/acp-7-2435-2007, 2007.

Sullivan, A., Peltier, R. E., Brock, C. A., de Gouw, J. A., Holloway, J. S., Warneke, C., Wollny, A. G., and Weber, R. J.: Airborne measurements of carbonaceous aerosol soluble in water over northeastern United States: Method development and an investigation into water-soluble organic carbon sources, J. Geophys. Res., 111, D23S46, doi:10.1029/2006JD007072, 2006.

Tang, I. N.: Thermodynamic and optical properties of mixed-salt aerosols of atmospheric importance, J. Geophys. Res., 102, 1883–1893, 1997.

Tang, I. N., Tridico, A., and Fung, K.: Thermodynamic and optical properties of sea salt aerosols, J. Geophys. Res., 102, 23,269–23,275, 1997.

Tang, Y., Carmichael, G. R., Uno, I., Woo, J-H., Kurata, G., Lefer, B., Shetter, R. E., Huang, H., Anderson, B. E., Avery, M. A., Clarke, A. D. and Blake, D. R.: Impacts of aerosols and clouds on photolysis frequencies and photochemistry during TRACE-P: 2. Three-dimensional study using a regional chemical transport model, J. Geophys. Res., 108(D21), 8822, doi:10.1029/2002JD003100, 2003.

Tian, J., Riemer, N., West, M., Pfaffenberger, L., Schlager, H., and Petzold, A.: Modeling the evolution of aerosol particles in a ship plume using PartMC-MOSAIC, Atmos. Chem. Phys., 14, 5327–5347, 2014.

Tie, X., Madronich, S., Walters, S., Edwards, D. P., Ginoux, P., Mahowald, N., Zhang, R., Lou, C., and Brasseur, G.: Assessment of the global impact of aerosols on tropospheric oxidants, J. Geophys. Res., 110, D03204, doi:10.1029/2004JD005359, 2005.

Toon, O. B.: An Overview of the 'Studies of Emissions and Atmospheric Composition, Clouds and Climate Coupling by Regional Surveys' (SEAC4RS) Field Mission (Invited) American Geophysical Union, Fall Meeting 2013, Abstract #A12D-01, 2013.

Toon, O., and Ackerman, T.: Algorithms for the calculation of scattering by stratified spheres, Applied Optics, 20, 3657–3660, 1981.

Virkkula, A.: Correction of the Calibration of the 3-wavelength Particle Soot Absorption Photometer (3λ PSAP), Aerosol Science and Technology, 44, 706–712, doi:10.1080/02786826.2010.482110, 2010.

Wang, J., Christopher, S. A., Brechtel, F., Kim, J., Schmid, B., Redemann, J., Russell, P. B., Quinn, P., and Holben, B. N.: Geostationary satellite retrievals of aerosol optical thickness during ACE-Asia, J. Geophys. Res., 108, 8657, doi:10.1029/2003JD003580, D23, 2003a.

Wang, J., Christopher, S. A., Reid, J. S., Maring, H., Savoie, D., Holben, B. N., Livingston, J. M., Russell, P. B., and Yang, S.-K.: GOES 8 retrieval of dust aerosol optical thickness over the Atlantic Ocean during PRIDE, J. Geophys. Res., 108, 8595, doi:10.1029/2002JD002494, D19, 2003b.

Wang, X., Heald, C. L., Ridley, D. A., Schwarz, J. P., Spackman, J. R., Perring, A. E., Coe, H., Liu, D., and Clarke, A. D.: Exploiting simultaneous observational constraints on mass and absorption to estimate the global direct radiative forcing of black carbon and brown carbon, Atmos. Chem. Phys., 14, 10989–11010, doi:10.5194/acp-14-10989-2014, 2014.

Wex, H., Neusüß, C., Wendisch, M., Stratmann, F., Koziar, C., Keil, A., Wiedensohler, A., and Ebert, M.: Particle scattering, backscattering, and absorption coefficients: An in situ closure and sensitivity study, J. Geophys. Res., 107, 8122, doi:10.1029/2000JD000234, 2002.

Yang, H. and Levy, H.: Sensitivity of photodissociation rate coefficients and O_3 photochemical tendencies to aerosols and clouds, J. Geophys. Res., 109, D24301, doi:10.1029/2004JD005032, 2004.

Matthew Alvarado 5/25/2016 3:01 PM
Formatted: Font:Not Italic

Matthew Alvarado 5/25/2016 3:01 PM
Formatted: Font:Not Italic

Matthew Alvarado 5/25/2016 3:01 PM
Formatted: Font:Not Italic

Matthew Alvarado 5/25/2016 3:01 PM
Formatted: Font:Not Italic

Matthew Alvarado 5/25/2016 3:01 PM
Formatted: Font:Not Italic

Matthew Alvarado 5/25/2016 3:01 PM
Formatted: Font:Not Italic

Matthew Alvarado 5/25/2016 3:01 PM
Formatted: Font:Not Italic

Matthew Alvarado 5/25/2016 3:01 PM
Formatted: Font:Not Italic

Unknown
Field Code Changed

Matthew Alvarado 5/25/2016 3:01 PM
Formatted: Font:Not Italic

Matthew Alvarado 5/25/2016 3:01 PM
Formatted: Font:Not Italic

Table 1. Lognormal mode parameters (r_g in µm, σ unitless), density (ρ, g cm^{-3}) and refractive indices (n, unitless) at 550 nm and 0% RH of selected aerosol types from OPAC v3.1, GMI, GEOS-Chem v9-02, and GC-RT.

Model	Parameter	BC/Soot	OC/WASO	Sea Salt (Acc. Mode)	Trop. Sulfate
OPAC v3.1	r_g	0.0118	0.0212	0.2090	0.0695
	σ	2.00	2.24	2.03	2.03
	ρ	1.0	1.8	2.2	1.7
	n	$1.75-0.44i$	$1.53-0.006i$	$1.50-10^{-8}i$	$1.43-10^{-8}i$
GMI	r_g	0.0118	0.0212	0.2090	0.05
	σ	2.0	2.0	2.0	2.0
	ρ	1.5	1.5	2.2	1.769
	n	$1.75-0.44i$	$1.53-0.006i$	$1.50-10^{-8}i$	$1.43-10^{-8}i$
GEOS-Chem v9-02	r_g	0.02	0.063	0.09	0.07
	σ	1.6	1.6	1.5	1.6
	ρ	1.0	1.8	2.2	1.7
	n	$1.75-0.44i$	$1.53-0.006i$	$1.50-10^{-8}i$	$1.53-0.01i$
GC-RT[a]	r_g	0.02	0.063	0.09	0.07
	σ	1.6	1.6	1.5	1.6
	ρ	1.8	1.8	2.2	1.7
	n	$1.95-0.79i$	$1.53-0.006i$	$1.50-10^{-8}i$	$1.53-0.01i$

[a] Baseline GC-RT configuration as described in Wang et al. (2014).

Table 2. Summary of results for modeling the submicron scattering coefficient throughout the entire ARCTAS campaign with OPAC v3.1, GMI, GEOS-Chem v9-02, and GC-RT. The mean (μ) and standard deviation (σ) of the $\log_{10}$ error distributions are shown. The correlation coefficient (r^2) and slope of the linear fit between the modeled and measured values are shown as well.

Wavelength	Metric	OPAC v3.1	GMI	GEOS-Chem v9-02	GC-RT[a]
450 nm	$\mu \pm \sigma$	0.07 ± 0.24	0.06 ± 0.24	0.15 ± 0.25	0.15 ± 0.24
	r^2	0.74	0.74	0.72	0.73
	Slope	0.89 ± 0.02	0.91 ± 0.02	1.01 ± 0.02	1.05 ± 0.02
550 nm	$\mu \pm \sigma$	0.15 ± 0.24	0.09 ± 0.24	0.17 ± 0.25	0.16 ± 0.24
	r^2	0.72	0.72	0.72	0.73
	Slope	0.95 ± 0.02	0.94 ± 0.02	1.05 ± 0.02	1.08 ± 0.03
700 nm	$\mu \pm \sigma$	0.27 ± 0.25	-0.05 ± 0.27	-0.04 ± 0.24	-0.09 ± 0.25
	r^2	0.70	0.58	0.72	0.71
	Slope	1.19 ± 0.03	0.63 ± 0.01	0.68 ± 0.02	0.63 ± 0.02

[a] Baseline GC-RT configuration as described in Wang et al. (2014).

Table 3. Summary of results for modeling the submicron absorption coefficient (using the correction of Lack et al., 2008) throughout the entire ARCTAS campaign with OPAC v3.1, GMI, GEOS-Chem v9-02, and GC-RT. The mean (μ) and standard deviation (σ) of the $\log_{10}$ error distributions are shown. The correlation coefficient (r^2) and slope of the linear fit between the modeled and measured values are shown as well.

Wavelength	Metric	OPAC v3.1	GMI	GEOS-Chem v9-02	GC-RT[a]
470 nm	$\mu \pm \sigma$	0.12 ± 0.28	0.04 ± 0.27	0.26 ± 0.26	0.20 ± 0.26
	r^2	0.70	0.72	0.69	0.70
	Slope	0.81 ± 0.06	0.83 ± 0.04	1.09 ± 0.05	0.96 ± 0.04
532 nm	$\mu \pm \sigma$	0.28 ± 0.29	0.06 ± 0.27	0.27 ± 0.25	0.22 ± 0.25
	r^2	0.70	0.71	0.68	0.69
	Slope	0.94 ± 0.06	0.94 ± 0.05	1.21 ± 0.06	1.07 ± 0.06
660 nm	$\mu \pm \sigma$	0.14 ± 0.29	0.00 ± 0.24	0.15 ± 0.25	0.09 ± 0.24
	r^2	0.68	0.68	0.65	0.67
	Slope	0.99 ± 0.10	0.75 ± 0.04	0.95 ± 0.06	0.84 ± 0.05

[a] Baseline GC-RT configuration as described in Wang et al. (2014).

Table 4. Summary of results for modeling the submicron single scattering albedo (SSA, using the correction of Lack et al., 2008) throughout the entire ARCTAS campaign with OPAC v3.1, GMI, GEOS-Chem v9-02, and GC-RT. The mean (μ) and standard deviation (σ) of the absolute error distributions are shown. The correlation coefficient (r^2) and slope of the linear fit between the modeled and measured values are shown as well.

Wavelength	Metric	OPAC v3.1	GMI	GEOS-Chem v9-02	GC-RT[a]
	$\mu \pm \sigma$	-0.01 ± 0.05	0.01 ± 0.05	-0.01 ± 0.05	0.00 ± 0.05
450 nm	r^2	0.17	0.07	0.09	0.10
	Slope	0.44 ± 0.03	0.65 ± 0.05	0.70 ± 0.04	0.61 ± 0.04
	$\mu \pm \sigma$	-0.01 ± 0.05	0.01 ± 0.05	-0.01 ± 0.05	-0.01 ± 0.05
550 nm	r^2	0.15	0.06	0.10	0.10
	Slope	0.43 ± 0.04	0.69 ± 0.06	0.73 ± 0.04	0.66 ± 0.04
	$\mu \pm \sigma$	0.01 ± 0.06	0.02 ± 0.07	-0.02 ± 0.06	-0.02 ± 0.06
700 nm	r^2	0.14	0.03	0.11	0.10
	Slope	0.32 ± 0.02	0.78 ± 0.14	0.79 ± 0.04	0.81 ± 0.04

[a] Baseline GC-RT configuration as described in Wang et al. (2014).

Table 5.Summary of results for modeling the submicron scattering coefficient throughout the entire ARCTAS campaign for ASP v2.1 using different mixing rules. The mean (μ) and standard deviation (σ) of the $\log_{10}$ error distributions are shown. The correlation coefficient (r^2) and slope of the linear fit between the modeled and measured values are shown as well.

Matthew Alvarado 5/24/2016 3:09 PM
Deleted: states

Wavelength	Metric	ASP v2.1 CS	ASP v2.1 EXT	ASP v2.1 VA	ASP v2.1 MG
450 nm	μ ± σ	-0.03 ± 0.17	-0.02 ± 0.17	-0.03 ± 0.17	-0.03 ± 0.17
	r^2	0.89	0.89	0.89	0.89
	Slope	0.99 ± 0.02	1.01 ± 0.02	0.99 ± 0.02	1.00 ± 0.02
550 nm	μ ± σ	-0.03 ± 0.17	-0.02 ± 0.17	-0.03 ± 0.17	-0.03 ± 0.17
	r^2	0.89	0.89	0.89	0.89
	Slope	1.00 ± 0.02	1.02 ± 0.02	1.00 ± 0.02	1.01 ± 0.02
700 nm	μ ± σ	-0.01 ± 0.17	0.00 ± 0.17	-0.01 ± 0.17	0.00 ± 0.17
	r^2	0.88	0.88	0.88	0.88
	Slope	1.07 ± 0.03	1.10 ± 0.03	1.08 ± 0.03	1.08 ± 0.03

Table 6. Summary of results for modeling the submicron absorption coefficient (using the correction of Lack et al., 2008) throughout the entire ARCTAS campaign for ASP v2.1 using different mixing rules. The mean (μ) and standard deviation (σ) of the $\log_{10}$ error distributions are shown. The correlation coefficient (r^2) and slope of the linear fit between the modeled and measured values are shown as well.

Matthew Alvarado 5/24/2016 3:09 PM
Deleted: states

Wavelength	Metric	ASP v2.1 CS	ASP v2.1 EXT	ASP v2.1 VA	ASP v2.1 MG	ASP v2.1 Variable
470 nm	$\mu \pm \sigma$	0.11 ± 0.32	-0.10 ± 0.32	0.16 ± 0.30	0.07 ± 0.32	0.04 ± 0.28
	r^2	0.47	0.50	0.47	0.47	0.45
	Slope	0.85 ± 0.09	0.54 ± 0.06	0.90 ± 0.09	0.79 ± 0.08	0.60 ± 0.08
532 nm	$\mu \pm \sigma$	0.13 ± 0.32	-0.05 ± 0.31	0.17 ± 0.30	0.09 ± 0.32	0.07 ± 0.28
	r^2	0.46	0.48	0.47	0.47	0.44
	Slope	0.93 ± 0.12	0.62 ± 0.09	0.98 ± 0.13	0.85 ± 0.11	0.68 ± 0.11
660 nm	$\mu \pm \sigma$	0.13 ± 0.32	0.00 ± 0.32	0.17 ± 0.30	0.09 ± 0.32	0.09 ± 0.29
	r^2	0.46	0.47	0.46	0.46	0.44
	Slope	0.97 ± 0.16	0.72 ± 0.13	1.02 ± 0.16	0.89 ± 0.14	0.76 ± 0.14

Table 7. Summary of results for modeling the SSA (using the correction of Lack et al., 2008) throughout the entire ARCTAS campaign for ASP v2.1 using different mixing rules. The mean (μ) and standard deviation (σ) of the absolute error distributions are shown. The correlation coefficient (r^2) and slope of the linear fit between the modeled and measured values are shown as well.

Matthew Alvarado 5/24/2016 3:09 PM
Deleted: states

Wavelength	Metric	ASP v2.1 CS	ASP v2.1 EXT	ASP v2.1 VA	ASP v2.1 MG	ASP v2.1 Variable
450 nm	μ ± σ	-0.02 ± 0.04	0.01 ± 0.03	-0.03 ± 0.04	-0.01 ± 0.04	-0.01 ± 0.04
	r^2	0.20	0.18	0.24	0.20	0.30
	Slope	0.51 ± 0.06	0.30 ± 0.03	0.64 ± 0.07	0.46 ± 0.05	0.61 ± 0.06
550 nm	μ ± σ	-0.04 ± 0.04	-0.01 ± 0.03	-0.04 ± 0.04	-0.03 ± 0.04	-0.03 ± 0.04
	r^2	0.20	0.17	0.25	0.20	0.30
	Slope	0.54 ± 0.06	0.32 ± 0.03	0.67 ± 0.06	0.48 ± 0.05	0.64 ± 0.06
700 nm	μ ± σ	-0.02 ± 0.05	0.00 ± 0.05	-0.03 ± 0.05	-0.01 ± 0.05	-0.01 ± 0.05
	r^2	0.17	0.13	0.22	0.16	0.25
	Slope	0.44 ± 0.05	0.28 ± 0.03	0.55 ± 0.05	0.38 ± 0.04	0.52 ± 0.05

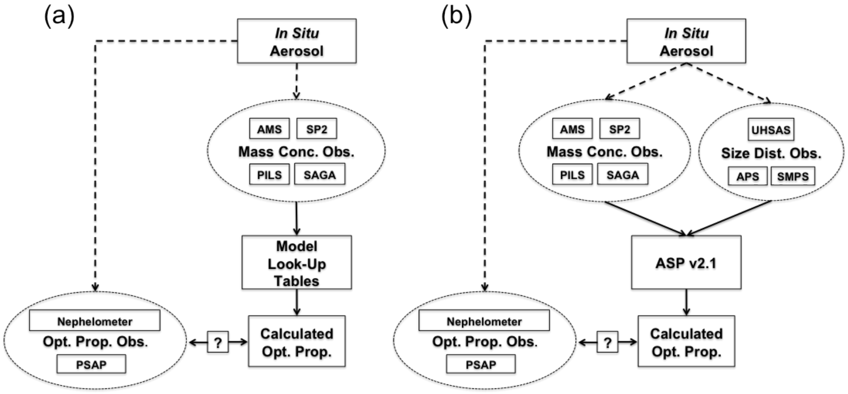

Figure 1. (a) Schematic of aerosol optical property closure study methodology for the OPAC v3.1, NASA GMI Combo model, GEOS-Chem v9-02, and baseline GC-RT aerosol parameterizations. (b) Schematic of closure study for ASP v2.1.

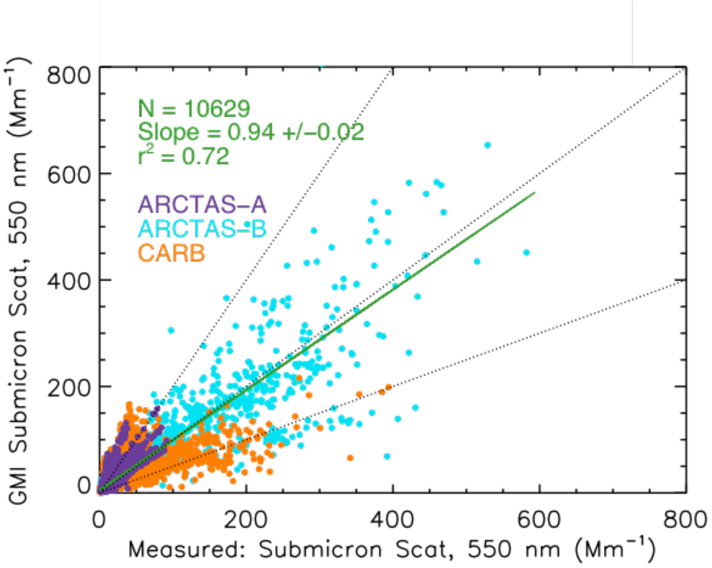

Figure 2. Example scatterplot of the measured submicron scattering coefficient (Mm^{-1}) at 550 nm versus the calculated submicron scattering coefficient for the GMI model. The color of the data points corresponds to the phase of the ARCTAS campaign (ARCTAS-A in purple, ARCTAS-B in cyan, and ARCTAS–CARB in orange). The dotted black lines are the 1:1 line, 2:1 line, and 1:2 line. The green line is the linear fit to the data. The number of data points (*N*), the slope of the linear fit, and the correlation coefficient (r^2) are shown as well.

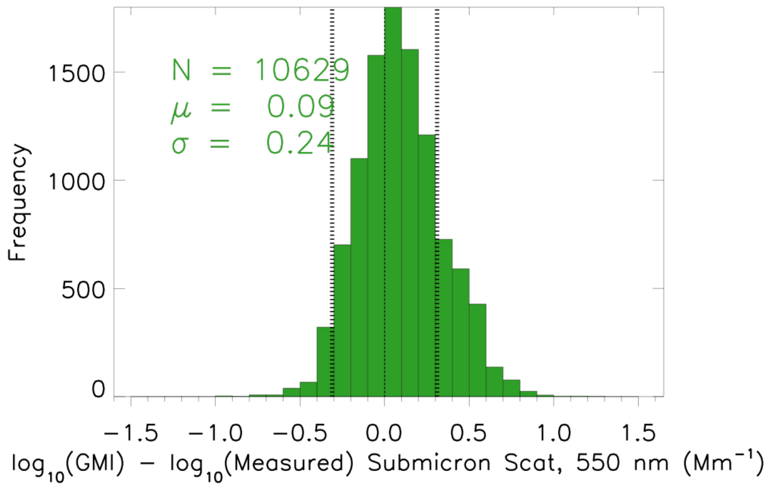

Figure 3. Example histogram of the errors in the $\log_{10}$ of the submicron scattering coefficient (modeled value – measured value) at 550 nm for the GMI model. The vertical dashed lines are at ± 0.31, corresponding to an error of a factor of 2. The number of data points (*N*) and the mean (μ) and standard deviation (σ) of the error distribution are also shown.

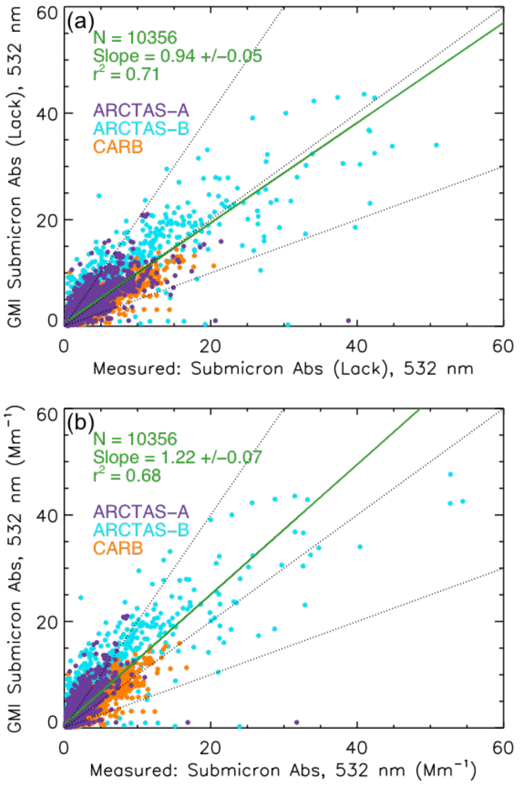

Figure 4. As in Figure 2, but for submicron aerosol absorption coefficients (Mm^{-1}) at 532 nm. The PSAP measured aerosol absorption has been corrected following (a) Lack et al. (2008) and (b) Virkkula (2010).

Matthew Alvarado 11/17/2015 3:28 PM

Deleted: Figure 2

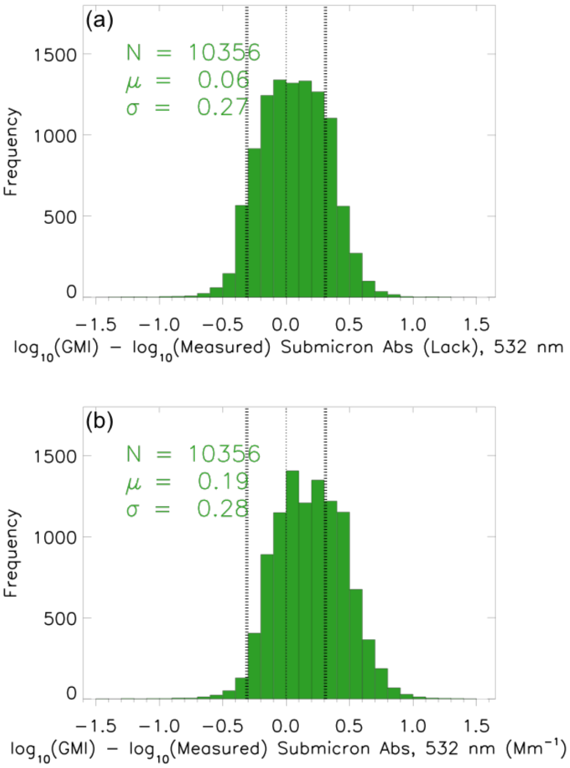

Figure 5. As in Figure 3, but for submicron aerosol absorption coefficients (Mm^{-1}) at 532 nm. The PSAP measured aerosol absorption has been corrected following (a) Lack et al. (2008) and (b) Virkkula (2010).

Matthew Alvarado 11/17/2015 3:28 PM
Deleted: Figure 3

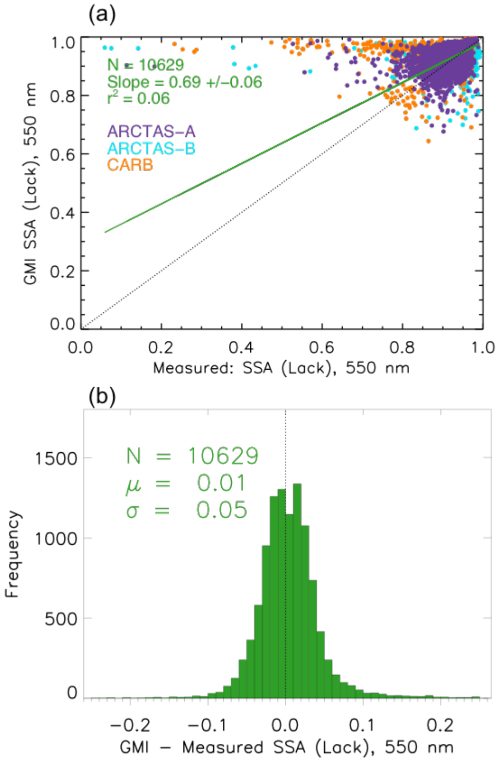

Figure 6. (a) Scatterplot of the measured submicron single scattering albedo (SSA) at 550 nm versus the calculated submicron SSA for the GMI model. The dotted black line is the 1:1 line. The green line is the linear fit to the data. (b) Histogram of the errors in the SSA (modeled value – measured value) at 550 nm for the GMI model.

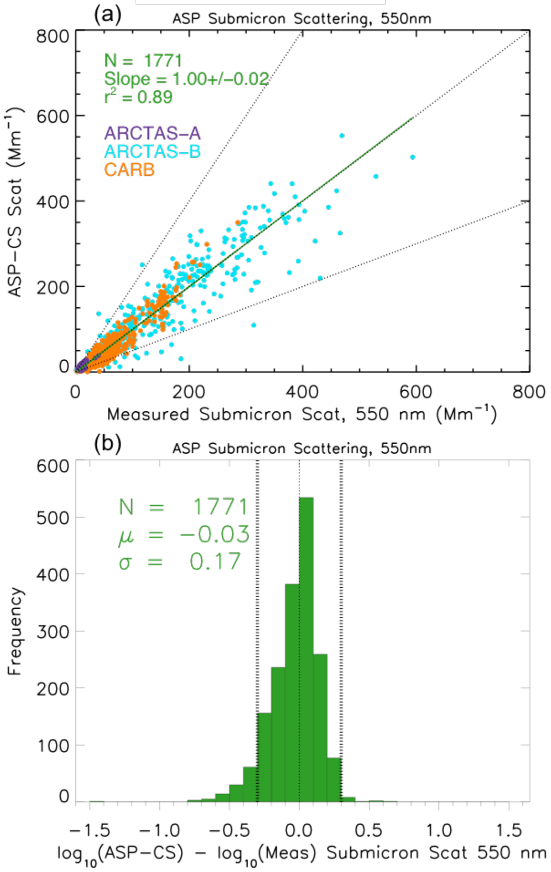

Figure 7. (a) Scatterplot of the measured submicron scattering coefficient (Mm^{-1}) at 550 nm versus the calculated submicron scattering coefficient for ASP v2.1. The dotted black lines are the 1:1, 2:1, and 1:2 lines. The green line is the linear fit to the data. Results for core-shell (CS) mixing rule are shown, but the results for other mixing rules are similar (see Table 5). (b) Histogram of the errors in the $\log_{10}$ of the submicron scattering coefficient (modeled value – measured value) at 550 nm for ASP v2.1. The vertical dashed lines are at ± 0.31, corresponding to an error of a factor of 2.

Matthew Alvarado 5/24/2016 3:09 PM
Deleted: state

Matthew Alvarado 5/24/2016 3:09 PM
Deleted: states

Matthew Alvarado 11/17/2015 3:28 PM
Deleted: Table 5

(a) ASP Submicron Abs, 532nm (Lack Correction)

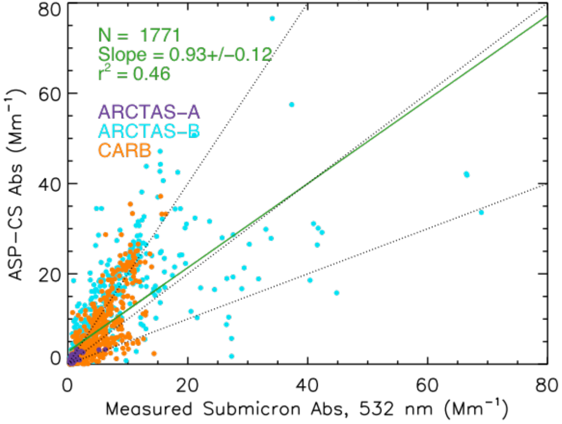

(b) ASP Submicron Abs, 532nm (Lack Correction)

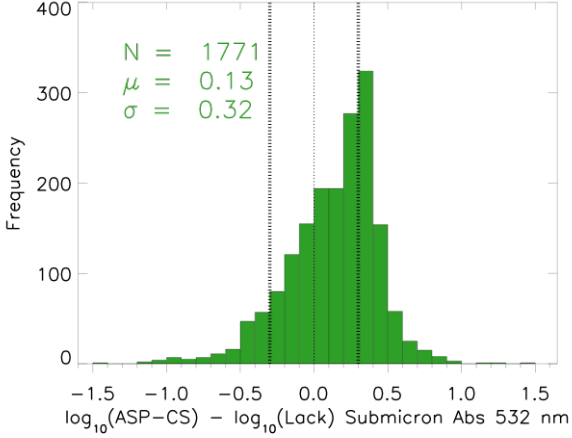

Figure 8. (a) Scatterplot of the measured submicron absorption coefficient (Mm^{-1}) at 532 nm versus the calculated submicron absorption coefficient for ASP v2.1. These results use the core-shell (CS) mixing rule. (b) Histogram of the errors in the log$_{10}$ of the submicron absorption coefficient (modeled value – measured value) at 550 nm for ASP v2.1 with the CS mixing rule.

Matthew Alvarado 5/24/2016 3:10 PM
Deleted: state

Matthew Alvarado 5/24/2016 3:10 PM
Deleted: state

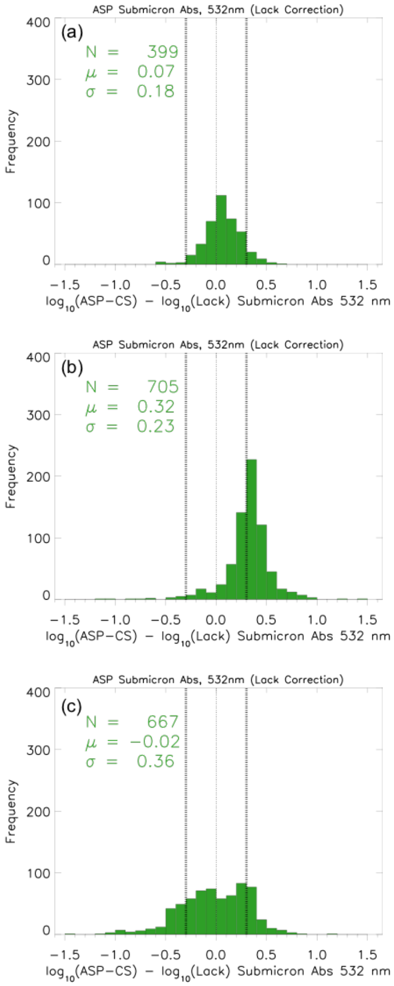

Figure 9. Histogram of the errors in the $\log_{10}$ of the submicron absorption coefficient (modeled value – measured value) at 550 nm for ASP v2.1 with the CS mixing rule. The PSAP measured aerosol absorption has been corrected following Lack et al. (2008). Results are broken apart for (a) ARCTAS-A, (b) ARCTAS-B, and (c) ARCTAS-CARB.

Matthew Alvarado 5/24/2016 3:10 PM
Deleted: state

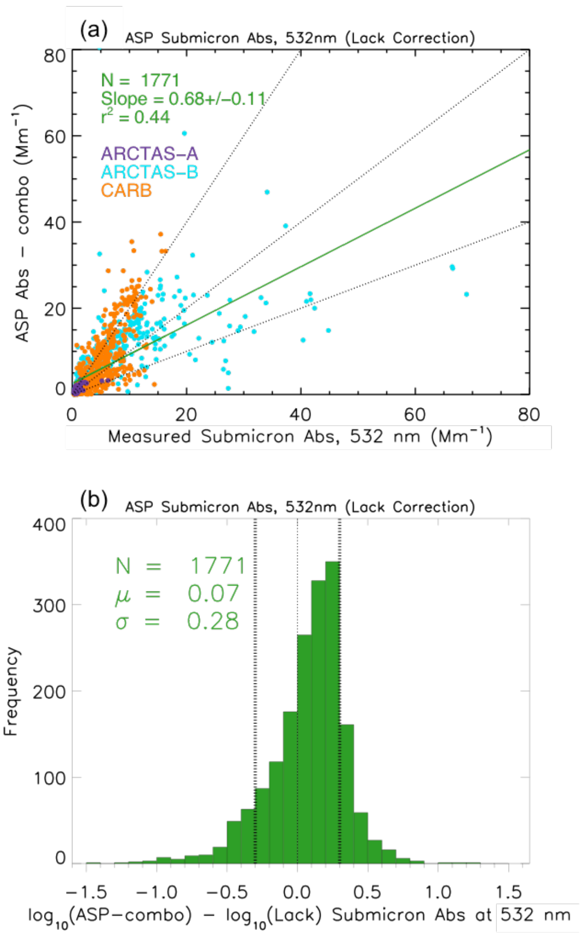

Figure 10. (a) As in Figure 8a, but using a variable mixing rule - core-shell (CS) is used for ARCTAS-A and ARCTAS-CARB, while an external mixture (EXT) is used for ARCTAS-B. (b) As in Figure 8b but with this variable mixing rule.

Matthew Alvarado 11/17/2015 3:28 PM
Deleted: Figure 8

Matthew Alvarado 5/24/2016 3:10 PM
Deleted: state

Matthew Alvarado 11/17/2015 3:28 PM
Deleted: Figure 8

Matthew Alvarado 5/24/2016 3:10 PM
Deleted: state